

2013

IMPROVING THE EFFICIENCY OF SOLAR PHOTOVOLTAIC POWER SYSTEM

Henry A. Aribisala
University of Rhode Island, aribisala@yahoo.com

Follow this and additional works at: <https://digitalcommons.uri.edu/theses>

Terms of Use

All rights reserved under copyright.

Recommended Citation

Aribisala, Henry A., "IMPROVING THE EFFICIENCY OF SOLAR PHOTOVOLTAIC POWER SYSTEM" (2013).
Open Access Master's Theses. Paper 161.
<https://digitalcommons.uri.edu/theses/161>

This Thesis is brought to you by the University of Rhode Island. It has been accepted for inclusion in Open Access Master's Theses by an authorized administrator of DigitalCommons@URI. For more information, please contact digitalcommons-group@uri.edu. For permission to reuse copyrighted content, contact the author directly.

IMPROVING THE EFFICIENCY OF SOLAR
PHOTOVOLTAIC POWER SYSTEM

BY

HENRY A. ARIBISALA

A THESIS SUBMITTED IN PARTIAL FULFILLMENT OF THE
REQUIREMENTS FOR THE DEGREE OF
MASTER OF SCIENCE
IN
ELECTRICAL ENGINEERING

UNIVERSITY OF RHODE ISLAND

2013

MASTER OF ELECTRICAL ENGINEERING DEGREE THESIS
OF
HENRY ARIBISALA

APPROVED:

Thesis Committee:

Major Professor: GODI FISCHER
 DAVID TAGGART
 HAIBO HE
 NASSER H. ZAWIA
 DEAN OF THE GRADUATE SCHOOL

UNIVERSITY OF RHODE ISLAND
2013

ABSTRACT

As the local and national clamor for foreign energy independent United States continues to grow unabated; renewable energy has been receiving increased focus and it's widely believed that it's not only the answer to ever increasing demand for energy in this country, but also the environmentally friendly means of meeting such demand. During the spring of 2010, I was involved with a 5KW solar power system design project; the project involved designing and building solar panels and associated accessories like the solar array mounts and Solar Inverter system. One of the key issues we ran into during the initial stage of the project was how to select efficient solar cells for panel building at a reasonable cost. While we were able to purchase good solar cells within our allocated budget, the issue of design for efficiency was not fully understood , not just in the contest of solar cells performance , but also in the overall system efficiency of the whole solar power system, hence the door was opened for this thesis. My thesis explored and expanded beyond the scope of the aforementioned project to research different avenues for improving the efficiency of solar photovoltaic power system from the solar cell level to the solar array mounting, array tracking and DC-AC inversion system techniques.

ACKNOWLEDGMENTS

I would like to express my deepest gratitude to my thesis advisor and the Chair of the Dept of Electrical, Computer and Biomedical Engineering, Dr. Godi Fischer, for his excellent guidance, patience, and for his ever- ready attitude to render help even when he's busy with many other very important things. I would like to thank Dr. David Taggart, the Chair of the Dept of Mechanical Engineering, who was very helpful not only for supervising the initial project that opens the door for this thesis, but also for introducing me to the mechanical laboratory staffs who were very helpful during the initial stage of this work. I will also like to thank Dr. Haibo He for agreeing to be a member of the thesis committee despite his tight schedules and for providing additional guidance towards the successful completion of the thesis. Sincere appreciation also goes to Dr. Shmuel Mardix of the Dept of Electrical, Computer and Biomedical Engineering for working with me during the initial phase of the thesis. I will also like to thank the department of Electrical, Computer and Biomedical Engineering (ECBE) and the URI as a whole for providing me with an excellent atmosphere for doing this research. The profound support from my Wife, my daughter Abiola, my siblings and my entire family cannot be overemphasized; I'm grateful to you guys. I'm also grateful to my parents, Chief David Aribisala and Chief (Mrs.) Esther Abiola Aribisala (Both of blessed memories) for their profound love and care.

Above all, I will like to thank the Almighty God, for his love and grace without which it would be impossible for me to have achieved any educational success let alone finishing this thesis, all Glory is to God and Father of The Lord Jesus Christ my Savior.

TABLE OF CONTENTS

| | |
|---|------------|
| ABSTRACT | ii |
| ACKNOWLEDGMENTS | iii |
| TABLE OF CONTENTS..... | iv |
| LIST OF TABLES | v |
| LIST OF FIGURES | vi |
| CHAPTER 1 | 1 |
| INTRODUCTION | 1 |
| CHAPTER 2 | 3 |
| REVIEW OF SEMICONDUCTOR PHYSICS OF SOLAR CELLS | 3 |
| CHAPTER 3 | 13 |
| IMPROVING THE EFFICIENCY OF SOLAR PHOTOVOLTAIC POWER SYSTEM..... | 13 |
| CHAPTER 4 | 53 |
| FINDINGS | 53 |
| CHAPTER 5 | 55 |
| CONCLUSION..... | 55 |
| BIBLIOGRAPHY | 57 |

LIST OF TABLES

| TABLE | PAGE |
|---|------|
| Table 1.1 Different solar cell performance Table- 2001 | 20 |
| Table 1.2 Azimuth Angle by heading..... | 28 |
| Table 1.3 PV-WATTS Simulation of the 5KW Power system: Fixed Array..... | 33 |
| Table 1.4 PV-WATTS Simulation of the 5KW Power system: 2-Axis Tracker | 34 |
| Table 1.5 Load Estimate of the 5KW power system | 36 |
| Table 1.6 Truth Table for output voltage and switching states..... | 44 |
| Table 1.7 Utility grid voltage and frequency limits for grid-tied PV | 46 |

LIST OF FIGURES

| FIGURE | PAGE |
|---|------|
| Figure 1.1 Typical Crystalline Silicon (cSi) Solar Cell. | 3 |
| Figure 1.2 a (P-type), b (N-type) and c (P&N-type) materials | 4 |
| Figure 1.3a Electrons and Holes migration at the PN-Junction. | 6 |
| Figure 1.3b PN-Junction and Depletion Region under equilibrium | 6 |
| Figure 1.4 Energy Band diagrams of a PN-Junction..... | 7 |
| Figure 1.5 Ideal Diode with no illumination and the equivalent circuit. | 8 |
| Figure 1.6 Incident light on a typical PN solar cell. | 10 |
| Figure 1.7 IV characteristic curves of a PN-Junction- dark and under illumination. .. | 11 |
| Figure 1.8 Solar Radiation Spectrums. | 16 |
| Figure 1.9 Solar Radiation Air Mass standards and corresponding Latitude | 17 |
| Figure 1.10 Solar Spectrums Terrestrial | 18 |
| Figure 1.11 Practical Solar Cell Equivalent circuit. | 20 |
| Figure 1.12 1 st Generation Solar Cells Efficiency Milestones | 22 |
| Figure 1.13 Amorphous Solar Cell | 23 |
| Figure 1.14 2 ND Generation Solar Cells Efficiency Milestones | 24 |
| Figure 1.15 3 RD Generations Solar Cells Efficiency Milestones | 25 |
| Figure 1.16 Best research Solar Cells Efficiency Milestones | 26 |
| Figure 1.17 Record 41.6% Efficient concentrator Solar Cells Efficiency | 27 |
| Figure 1.18 Sun's Position, Azimuth and Altitude | 28 |
| Figure 1.19 A 2-Axis Tracking System | 30 |

| FIGURE | PAGE |
|---|------|
| Figure 1.20 30W/2.5V Solar Panel | 32 |
| Figure 1.21 Plots of peak power at different tilt angles | 32 |
| Figure 1.22 PV-Watts analysis of the 5KW Project: Fixed Vs 2-Axis Tracker | 34 |
| Figure 1.23 Parallel connection of 17 (12V) Panels | 35 |
| Figure 1.24 12V/294W Handmade Solar Panel..... | 36 |
| Figure 1.25 Grid Interactive Photovoltaic Power system | 38 |
| Figure 1.26 2-Level 3-Phase Inverter Topology | 41 |
| Figure 1.27 3-Level 3-phase Inverter Topology | 42 |
| Figure 1.28 3-Level 3-Phase Inverter Topology (Phase 1) | 43 |
| Figure 1.29 MPP on IV-Curve of a PV module | 45 |
| Figure 1.30 Powerex 600A/600V Dual IGBT Module | 48 |
| Figure 1.31 Powerex 600A/600V Dual IGBT schematic | 49 |
| Figure 1.32 Harmonics of a 3-Phase Grid-tied Inverter system | 50 |
| Figure 1.33 3-Phase 300A Line Inductor | 51 |
| Figure 1.34 Snap picture of a 3-Phase 100KVA Transformer under Test | 52 |

CHAPTER 1

INTRODUCTION

Solar energy is clean and is abundantly available. Solar technologies use the sun to provide heat, light, electricity, etc for domestic and industrial applications. With the alarming rate of depletion of the major conventional energy resources such as Coal, Petroleum and Natural gas, coupled with the environmental degradation caused by the process of harnessing these energy sources, it has become an urgent necessity to invest in renewable energy resources that would power the future sufficiently without degrading the environment through green house gas emission. The energy potential of the sun is immense, but despite this unlimited solar energy resource, harvesting it is a challenge mainly because of the limited efficiency of the array cells. The best conversion efficiency of most commercially available solar cells is in the range 10-20s% [1], [8]. Although recent breakthrough in the technology of solar cells shows significant improvement but the fact that the maximum solar cell efficiency still falls in the less than 20s% range shows there are enormous room for improvement. The goal of this thesis is to identify these rooms and ways to improving them. One of such room is array mounting and tracking mechanism that moves or positions solar array to absorbing extended solar irradiance for maximum power output. Another such room is researching different types of solar cells from past to present and the future trend and identifies the sources of losses and how to mitigate them. Lastly, some critical

components that are necessary for efficient operation of solar power inverter system are investigated.

CHAPTER 2

REVIEW OF SEMICONDUCTOR DEVICE PHYSICS OF SOLAR CELLS

Solar Cell Device Physics:



Figure 1.1 Typical Crystalline Silicon (cSi) Solar Cell [1], [15]

Solar cell like the crystalline silicon based solar cell shown in Figure 1 above is a solid state semiconductor p-n junction device that converts sunlight into direct-current electricity through the principle of photo-voltaic effect. The first conventional photovoltaic cells were produced in the late 1950s, and were principally deployed to provide electrical power for orbital satellites. During this initial deployment, excessive

cost of manufacturing and poor efficiency of solar modules were some of the major challenges that limit their competitiveness as a major source for meeting the increasing energy demand that has continued till now. However, recent improvements in design, manufacturing, performance, reduced cost and quality of solar cells and modules have not only opened up the doors for their deployments in applications like powering remote terrestrial applications, rural electrification projects, battery charging for navigational aids, water pumping, telecommunications equipment and critical military installations, but has also propelled solar power system as a competitive means to meeting the ever increasing power need for the world economy. While the focus of this thesis is improving the efficiency of a solar power system, it's important to take some cursory, but refreshing look at the semiconductor physics of a solar cell.

Basic semiconductor physics of solar cells:

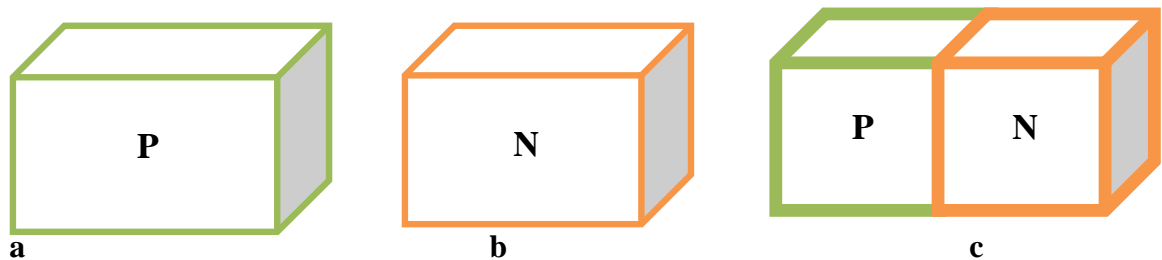


Figure 1.2: a (P-type), b (N-type), c (P & N type) Materials [1]

P-N Junction: Solar cell is simply a PN junction device, like a diode that is forward biased with a photo-voltage. Based on this simple definition, it's necessary to review how the PN-junction of a semiconductor diode functions. When a P-type and an N-type (Figure 1.2 above) semiconductors are interfaced together, PN junction is formed. The PN-Junction is the region or a boundary that is formed by doping or by epitaxial growth of a layer of crystal doped with one type of dopant on top of a layer of crystal.

A dopant is a material (Impurity) that is intentionally introduced or mixed into an extremely pure (Intrinsic or un-doped - Crystal Silicon for example) semiconductor material for the purpose of changing or optimizing its electrical properties for specific application. A dopant could be n-type or p-type material. Thus, a P-type Doping is the introduction of impurity atoms with one less valence electron- (Like Boron) than silicon (acceptor impurities), resulting in excess positive charge carriers (holes). Whereas, an N-type doping is the introduction of impurity atoms with one more valence electron (like Phosphorous) than silicon (donor impurities), resulting in excess negative charge carriers (electrons).

Figure 1.3a and b below shows a PN-junction without a bias, under this condition , electrons from the high concentration n-type side tends to flow towards the p-type side and similarly the holes from the high concentration p-type side tends to migrate towards the n-type side. These electron and holes migration creates charge imbalance by exposing ionized charges on both sides. The exposed charges would set up an electric field that opposes the natural diffusion tendency of the electron and holes at the junction; this is the behavior of the PN-Junction under equilibrium condition. Under this condition, there exists within the junction a layer between the PN-Junction that becomes almost completely depleted of mobile charge carriers. This layer/region is called the space-charge region or depleted region and is schematically illustrated in Figure 1.3b below.

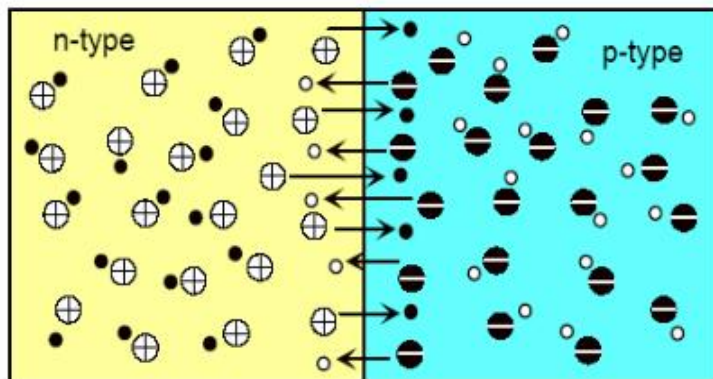


Figure 1.3a Electrons and Holes migration at the PN-Junction [16]

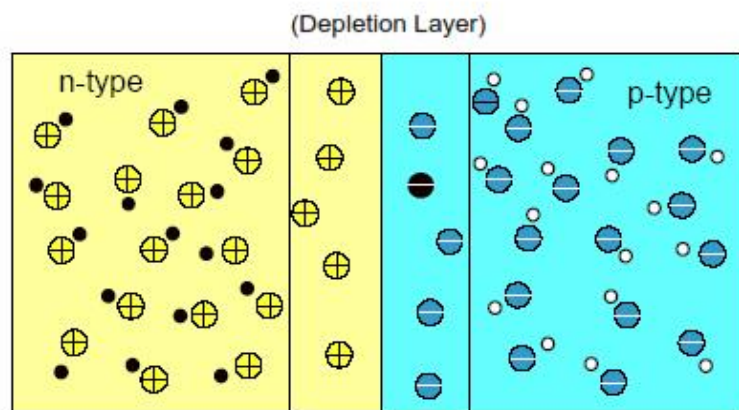


Figure 1.3b PN-Junction and Depletion Region under equilibrium [16]

The characteristic of the depletion layer is that the total amounts of charge on either side of the junction in the depletion region are equal and the net current flow is zero since the drift current and the diffusion charges are equal. Also the Fermi level is constant during this condition, but the width of the depletion layer can be altered if an external bias is applied. The junction barrier potential becomes increased if reversed biased and becomes narrower if forward biased. Figures 1.4 below shows the energy band diagram at equilibrium, forward bias and reverse bias conditions.

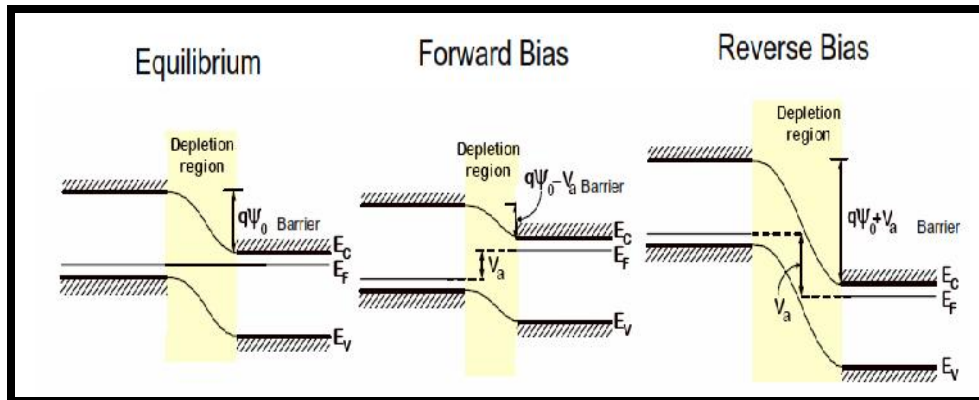


Figure 1.4 Energy Band diagrams of a PN-Junction [1], [16]

From Figure 1.4 above and as explained before, when no external force like voltage or excess heat or incident light is acting on the junction, electrons in the n-type material closest to the boundary tend to migrate, or diffuse into the p-type material, resulting in the creation of minority positively charged ions in the n-type material and negatively charged minority ions in the p-type material. The electric field developed by the displaced charges is referred to as the junction built-in potential and the region nearby the PN-junction loses their neutrality forming the depletion layer or space charge region. This is PN-junction in a state of equilibrium.

On the other hand if a voltage is applied across the P-N junction, with the positive terminal connected to the n-type material and the negative terminal connected to the p-type material, the junction is reverse biased; under this condition, the depletion region would further increase as the diffused electrons and holes are pulled further from the boundary and thus increasing the resistance of the material to the flow of current, but there will be a negligible flow of reverse current. The reverse current will remain constant and continue to flow until breakdown voltage is reached. However, if the positive terminal is connected to the p-type region and the negative connected to the n-

type material, the junction is forward biased. Now the solar cell operates similar to a forward biased diode.

Ideal Diode in the Dark and under Illumination:

In order to understand the operation of a solar cell, it is necessary to analyze the concepts of an ideal PN diode. In general, an ideal diode under dark conditions i.e. no illumination, will have a dark *I-V* characteristic and equation as given in equation 1 and Figure 1.5 below.

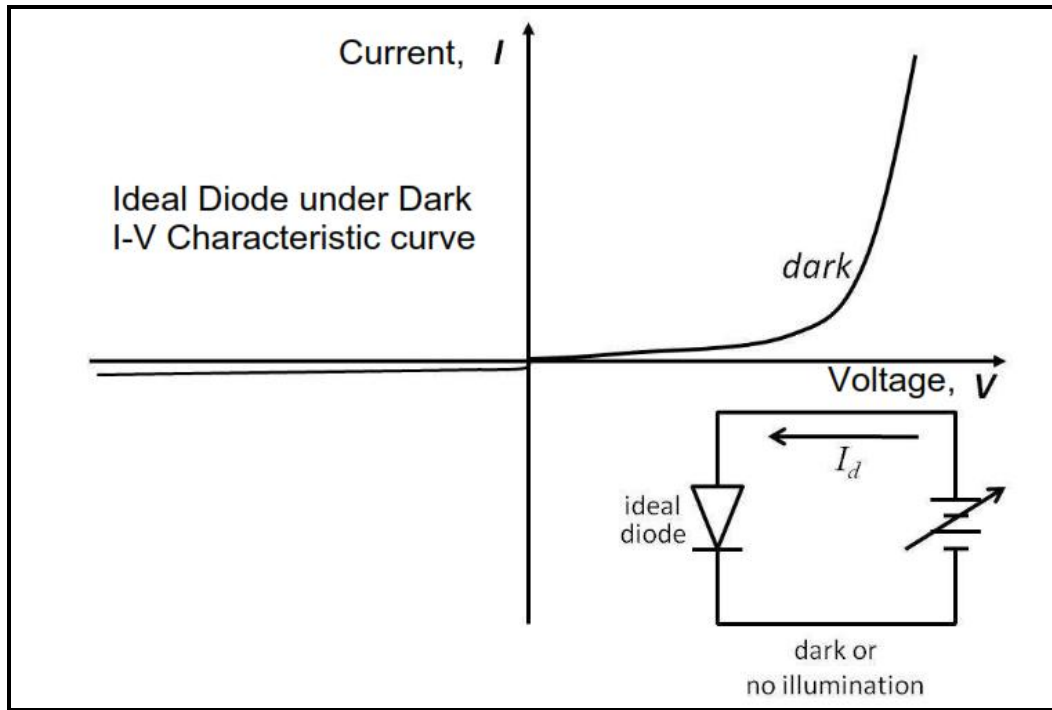


Figure 1.5: Ideal Diode with no illumination and the equivalent circuit: [1]

$$I = I_0 (e^{qV/KBT} - 1) \quad \text{----- 1}$$

Equation 1 is the ideal diode or Shockley equation Where;

I = the current through the diode,

I_0 = the diode saturation current density.

T = the absolute temperature °K,

k_B = the Boltzmann constant,

q= the electron charge and

V= the voltage between the two terminals of p-n ideal diode. Also the expression for the diode saturation current density I_o is given by equation 2 below;

$$I_o = qA \left(\frac{D_e}{L_e} * \frac{n_i \wedge 2}{N_A} + \frac{D_h}{L_h} * \frac{n_i \wedge 2}{N_D} \right) \text{ ----- 2}$$

Where;

A is the cross-sectional area of the PN-diode,

n_i is the number of electron hole-pairs ,

D_e is the electron diffusion coefficient

D_h is the hole diffusion coefficient

The minority carrier diffusion lengths, L_e and L_h are defined as follows;

$$L_e = \sqrt{D_e * \tau_e} \text{ ----- 3}$$

$$L_h = \sqrt{D_h * \tau_h} \text{ ----- 4}$$

τ_e and τ_h are the minority carrier material lifetime constants. Based on the above

equations, the diode saturation current is largely dependent on the structure and the material used for the manufacturing of the diode.

Ideal Solar Cell:

When a solar cell is illuminated by sun-light, (Figure 1. 6 below), photons energy of the incident light is converted to direct current electricity through the process of photovoltaic effect of the solar cell. Incident light causes electron-hole pairs to be generated in the semiconductor and there is increase in the concentration of minority

carriers (electrons in the p-type region and holes in the n-type region) in the depletion region. This increase in the concentration of minority carriers results in the flow of the minority carriers across the depletion region into the quasi-neutral regions. These photo-generated carriers cause the flow of photo-generated current, I_{photons} . When the junction is in the open-circuit condition, no net current can flow inside the p-n junction, thus the current resulting from the flux of photo-generated and thermally-generated carriers is balanced by the opposite recombination current.

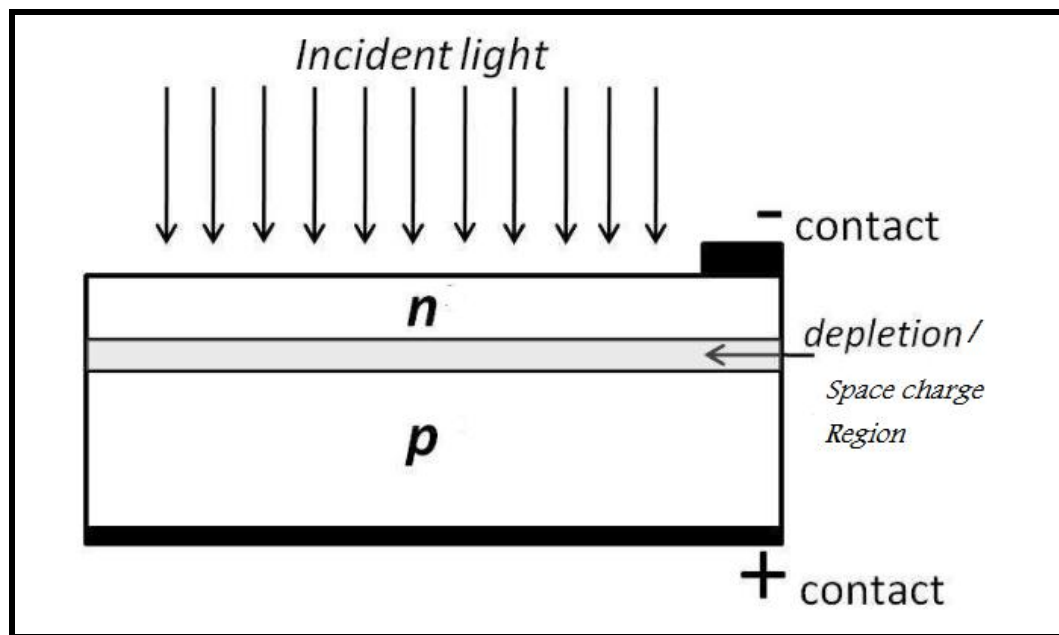


Figure 1.6 Incident light on a typical PN Solar Cell [28]

If a load is connected between the electrodes of the illuminated p-n junction, some fraction of the photo-generated current will flow through the external circuit. The potential difference between the n-type and p-type regions will be lowered by a voltage drop over the load. Also the electrostatic potential difference over the depletion region will be decreased which results in an increase of the recombination current. Applying superposition theorem, the net total current flowing through the load

is determined as the sum of the photo- and thermal generation currents and the recombination current as shown in the IV-characteristic curves (Figure 1.7) and the equation 3 below.

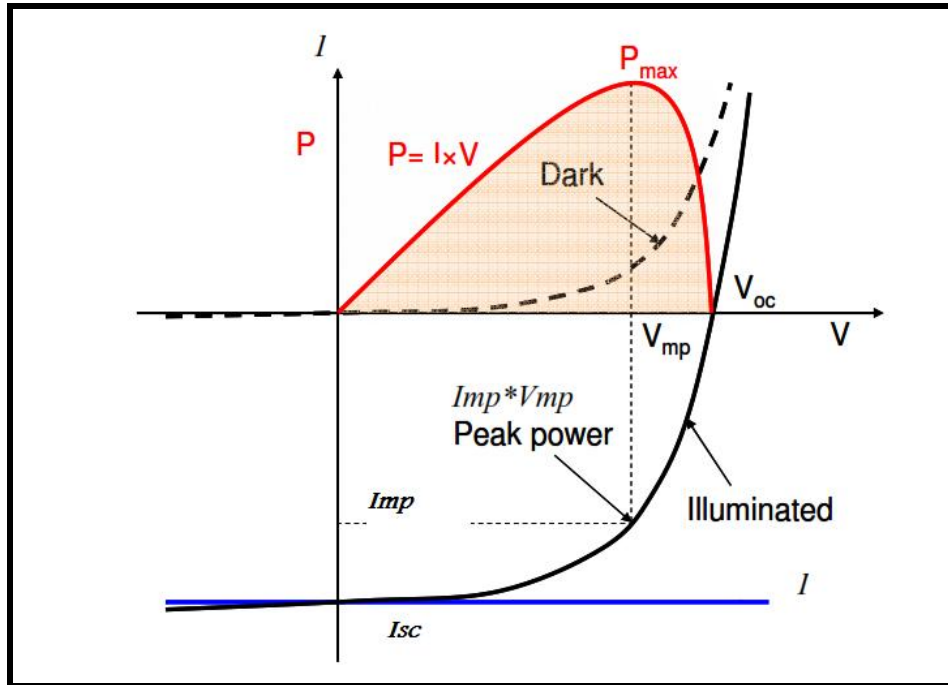


Figure 1.7 IV characteristic curves of a p-n junction in the dark and under illumination. [1], [27]

The PN-Junction IV characteristic curve of an ideal diode solar cell is described by the Shockley equation 3 below [1];

$$I = I_{\text{photon}} - I_0 (e^{qV/KBT} - 1) \quad \text{----- 5}$$

The Shockley equation is the fundamental device physics equation which describes the current-voltage behavior of an ideal p-n diode. I_{photon} is the photo-generated current and is defined by equation 4 below, [1].

$$I_{\text{photon}} = qAG(L_e + W + L_h) \quad \text{----- 6}$$

Where L_e and L_h as defined before are the minority carrier diffusion lengths for electron and holes respectively. G is the diode electron-hole pair generation rate, W is the width of the depletion layer and A is the total illuminated cross sectional area of the device. Based on this equation, it can be inferred that only carriers generated in the depletion region and in the regions up to the minority-carrier-diffusion length from the depletion region contributes to the photo-generated current.

CHAPTER 3

IMPROVING THE EFFICIENCY OF SOLAR PHOTOVOLTAIC POWER SYSTEM

Solar Cell Conversion Efficiency :

The conversion efficiency of a typical solar cell is the ratio of the maximum output generated power to the input or incident power. Certain output parameters greatly influences how efficient a solar cell is and are defined as follows.

Short circuit current I_{SC} : This is the current that flows through the external circuit when the electrodes of a solar cell are short circuited. The short-circuit current is dependent on the incident photon flux density and the spectrum of the incident light. The spectrum is standardized to the AM1.5 (see Figure 1.9 and 1.10 below) for standard solar cell parameter measurements. For Ideal solar cell, $I_{sc} = I_{\text{photon}}$. And this is the maximum current delivery capacity of the solar cell at any given illumination level. From Figure 1.10, the maximum I_{SC} is found by the integration of the spectrum distributions from low wavelengths up to the maximum wavelength at which electron-hole pairs can be generated for a given semiconductor. The common relationship between the wavelength and the photon energy is $E_{(eV)} = 1.24/\lambda$. Silicon has a band gap of 1.1eV and the λ corresponding to this is about 1.13 μm . Crystalline silicon solar cell can deliver a maximum of 46mA/cm² under an AM1.5 spectrum [1].

Open Circuit Voltage (V_{oc}):

The open-circuit voltage is the voltage at which no current flows through the external circuit; i.e. when the solar cell terminals are opened or not connected to a load. It is the maximum voltage that a solar cell can deliver under any given illumination. An ideal PN-Junction cell V_{oc} is given as follows in equation 7;

$$V_{oc} = \frac{K_B T}{q} \ln \left(\frac{I_{photon}}{I_o} + 1 \right) \text{ ----- } 7$$

From this equation, The V_{oc} depends on the photo-generated current density I_{photon} and the saturation current I_o . Also since the saturation current depends largely on the recombination in the solar cell, the open circuit voltage is a measure of the recombination in the device. For silicon solar cell, the maximum open circuit voltage is about 700mV.

Maximum Power (P_{MP}):

The Maximum current and voltage of a typical solar cell are represented at the 4th quadrant of the IV characteristic curve of Figure 1.6, the maximum power is the area of the product of the maximum current I_{mp} and Voltage V_{mp} as shown in the equation 8 below.

$$P_{MP} = V_{MP} * I_{MP} \text{ ----- } 8$$

Fill Factor FF:

The fill factor FF is the ratio of the maximum power (P_{MP}) generated by the solar cell to the product of the voltage open circuit V_{oc} and the short circuit current I_{sc}

$$FF = \frac{P_{MP}}{V_{oc} * I_{sc}} = \frac{V_{MP} * I_{MP}}{V_{oc} * I_{sc}} \text{-----} 9$$

From the above set of equations we define the solar cell **conversion efficiency** as the ratio of the maximum generated power ($P_{MP}=V_{MP} \cdot I_{MP}$) to the input or incident power P_{in} as given by equation 10 below.

$$\eta = \frac{V_{MP} * I_{MP}}{P_{in}} = \frac{V_{oc} * I_{sc} * FF}{P_{in}} \text{-----} 10$$

P_{in} is the total power of sunlight illumination on the cell. Energy-conversion efficiency of commercially available solar cells typically lies between 10 and 25 % [8]. These three important parameters (V_{oc} , I_{sc} and FF) as described above are the most important factors that determine how efficient a solar cell is and are optimized for efficient solar cell design.

Improving the Conversion Efficiency of Solar Cell:

This section identifies the major sources of loss in the solar cell conversion efficiency process and the corresponding approaches to mitigating the losses thereby improving the efficiency.

Light Energy (Photons) Absorption:

Sunlight is a portion of the electromagnetic radiation (Infrared, Visible and Ultraviolet lights) that is emitted by the Sun. On Earth, sunlight is filtered through the Earth's atmosphere, and is visible as daylight when the Sun is above the horizon. The amount

of radiant energy received from the Sun per unit area per unit time is called Solar Irradiance and it is a function of wavelength at a point outside the Earth's atmosphere. Solar irradiance is greatest at wavelengths of between 300-800 nm. Figure 1.8 below shows the solar spectrums. The spectrum of the Sun's solar radiation is very closely matches that of a black body with a temperature of about 5,800 deg K. [3]

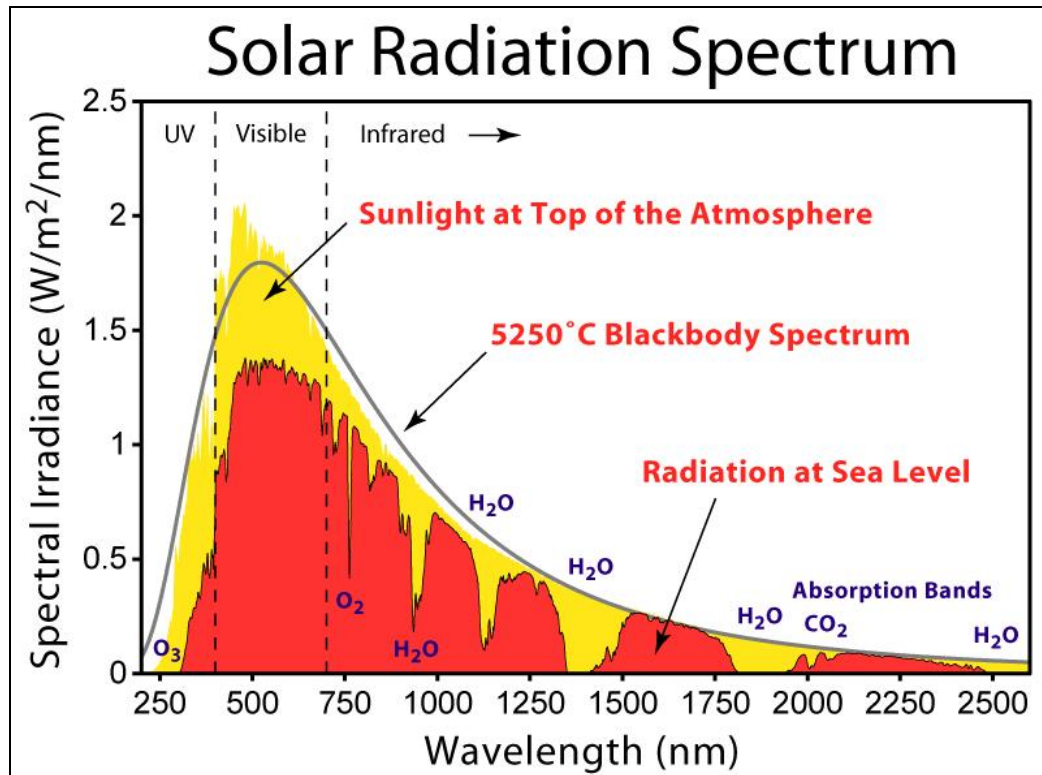


Figure 1.8 Solar Radiation Spectrums [2], [17]

The path length of the solar radiation through the Earth's atmosphere in units of Air Mass (AM) increases with the angle from the zenith. For a path length L through the atmosphere and solar radiation incident at angle θ relative to the normal to the Earth's surface, the air mass coefficient (AM) is;

$$AM = L/L_0 = 1/\cos \theta \quad \text{-----} \quad 11$$

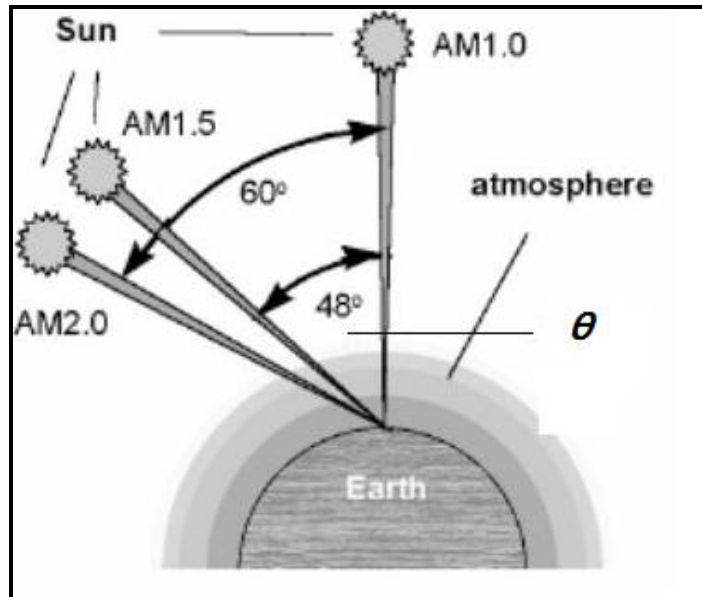


Figure 1.9 Solar Radiation Air Mass standards and corresponding Latitude [22]

The AM 1.5 spectrum which correspond to Latitude 48.2° is the preferred standard spectrum for solar cell efficiency measurements. Where L_0 (the zenith path length) is perpendicular to the Earth's surface at sea level and θ is the zenith angle in degrees. The air mass number is dependent on the Sun's elevation path through the sky and therefore varies with time of day and with the passing seasons of the year, and also with the latitude of the observer. At the outer space i.e. beyond our terrestrial environment, the solar spectrum has an Air Mass coefficient of zero (AM0) as seen in Figure 1.9 above and Figure 1.10 below

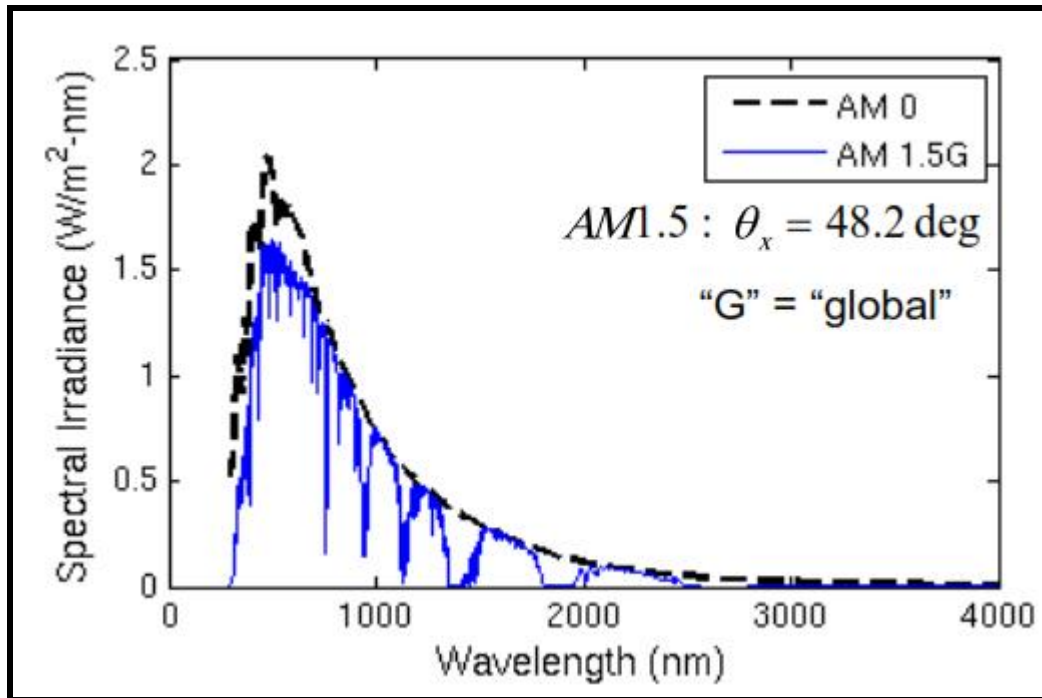


Figure 1.10 Solar Spectrums Terrestrial [2], [17]

The integrated power of the sun at AM0 spectrum is 136.6 mW/cm^2 [4]. Since the sun's radiation travels through the atmosphere and would encounter various atmospheric diffusion and attenuation, the solar spectrum Air mass coefficient from the surface of the earth atmosphere at typical latitude 48.2° is AM1.5G, the integrated power is reduced approximately to 100 mW/cm^2 [4]. This is the standard power that most solar cells conversion efficiency is measured against. This means for example, if a solar array produces a power output of 15 mW/cm^2 , then the conversion efficiency would be 15%.

The question then is how many photons can be absorbed per unit area of solar array? Let us consider silicon cell as example to answer this question; if we have a Silicon solar cell with energy band gap of $E = 1.1 \text{ eV}$. Only photons with energy greater than 1.1 eV and wavelength $< \text{bandgap}$, about $1.13 \mu\text{m}$ would be absorbed and the rest will

be lost as heat [28]. Also, even when the incident light with the adequate energy level and wavelength strikes the surface of the cell material, some photons are reflected from the surface of the solar cells; All these leads to reduced efficiency.

One way to ensure maximum absorption is through the use of cell material with very low reflective coefficient or placing a thin film anti-reflective coating over cell surface. Another method that can be employed in reducing reflection is using textured surface, in which the direction of reflected light on the textured surface is downward so that reflected photons can be reabsorbed again by the cell, thereby improving the conversion efficiency [28].

Losses Due to parasitic resistance:

Another source of loss is through parasitic resistance. The equivalent circuit of practical solar cell is shown in the Figure 1.11 below and the ideal diode equation 3 as modified below. This is different from the ideal solar cells because of the introduction of series resistance (R_s) which arises from the cell material surface to the contacts. Series resistance is worse at high photo-current. And the Shunt resistance (R_{sh}) arises from the leakage of current around the edges of the device and between contacts of different polarity. It is particularly profound with the cell material of poor rectifying characteristic. The effect of parasitic resistances is that it reduces the area of the maximum power rectangle ($V_{OC} \cdot I_{SC}$) of the IV characteristic curves and hence the efficiency suffers. However, latest cells manufacturing improvement and control of material chemistry has shown significant improvement in achieving optimum cell resistivity and thus improved efficiency. [18], [19]

$$I = I_L - I_0 \left(e^{q(V+IR_S)/KBT} - 1 \right) - \frac{V + IR_S}{R_{SH}} \quad \text{-----} \quad 12$$

Equations 1 through 12 [1]

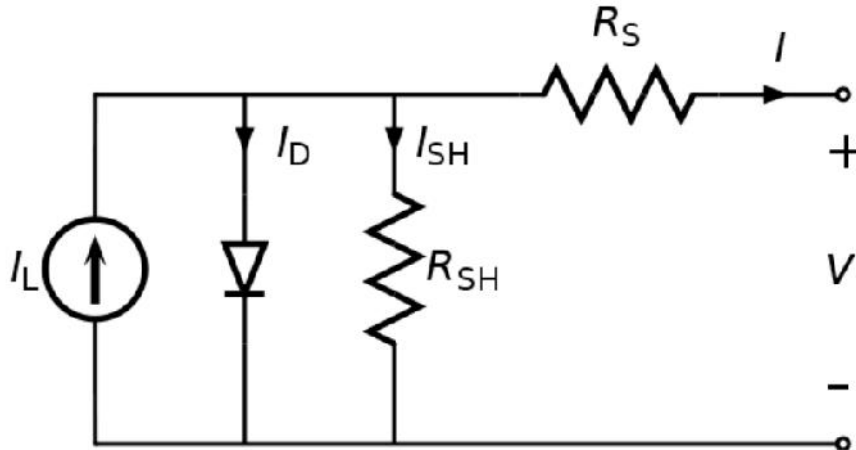


Figure 1.11 Practical Solar Cell Equivalent circuit. [17]

| Cell Type | Area (cm ²) | V _{oc} (V) | J _{sc} (mA/cm ²) | FF | Efficiency (%) |
|-----------------------|-------------------------|---------------------|---------------------------------------|------|----------------|
| crystalline Si | 4.0 | 0.706 | 42.2 | 82.8 | 24.7 |
| crystalline GaAs | 3.9 | 1.022 | 28.2 | 87.1 | 25.1 |
| poly-Si | 1.1 | 0.654 | 38.1 | 79.5 | 19.8 |
| a-Si | 1.0 | 0.887 | 19.4 | 74.1 | 12.7 |
| CuInGaSe ₂ | 1.0 | 0.669 | 35.7 | 77.0 | 18.4 |
| CdTe | 1.1 | 0.848 | 25.9 | 74.5 | 16.4 |

Table 1.1 Different Solar Cells performance table -2001 [6]

Evolution of Solar Cells:

1st Generation Solar Cells (Crystalline silicon (c-Si) PV technology):

Photovoltaic effect was first recognized by the French physicist, Alexandre-Edmond Becquerel in 1839, but the first modern solar cell with enough efficiency for power applications was not developed until 1954 at Bell Labs in New Jersey in 1954. While experimenting with semiconductors, Bell lab accidentally found that silicon doped

with certain impurities was very sensitive to light. This is the birth of 1st generation solar cell technology. It is Silicon-based technology and is the dominant technology in the commercial production of solar cells, accounting for more than 86% of the solar cell market. It is technically proven and reliable, and has succeeded in achieving market penetration, primarily in off-grid remote areas and lately in grid-connected applications. There are however, several inherent limitations to this 1st generation technology from the onset. Silicon wafers are very fragile and the process involved in the manufacturing is difficult and labor intensive, hence high cost. There are two approaches to manufacturing crystalline silicon based solar cells; single crystal and multi-crystalline cells. The Single crystal silicon wafers (c-Si) or the Mono-crystalline Solar Cells in which the crystal lattice of the entire sample is continuous and unbroken with no grain boundaries is still one of the most efficient photovoltaic solar cells to date. The process of production involves crystalline silicon rods being extracted from melted silicon and then sawed into thin plates. About half of the manufacturing cost comes from wafering; a time-consuming and costly batch process in which ingots are cut into thin wafers with a thickness of about 200 micrometers. If the wafers are too thin, the entire wafer will break in the process and due to this thickness requirement, a PV cell requires a significant amount of raw silicon and close to half of this not very inexpensive material is lost as sawdust in the wafer processes. The polycrystalline approach uses discrete cells on silicon wafers cut from multi-crystalline ribbons; the process is less expensive than the single crystalline cells. The average price for single-crystal modules is about \$3.97 per peak watt compare to \$2.43 for poly-crystal modules [6]. Though it is more expensive, Mono-crystalline silicon

cells are generally more durable and efficient and produce more wattage per square foot than their polycrystalline cell counterpart. Other advantages of crystalline silicon based solar cells are that they have broad spectral absorption range and high carrier mobility. The efficiency of mono-crystalline silicon solar cell currently peaks at about 28% while poly-crystalline cells are approaching about 20% [5]. Please see the chart below in Figure 1.12 for efficiency milestone of crystalline based solar cell.

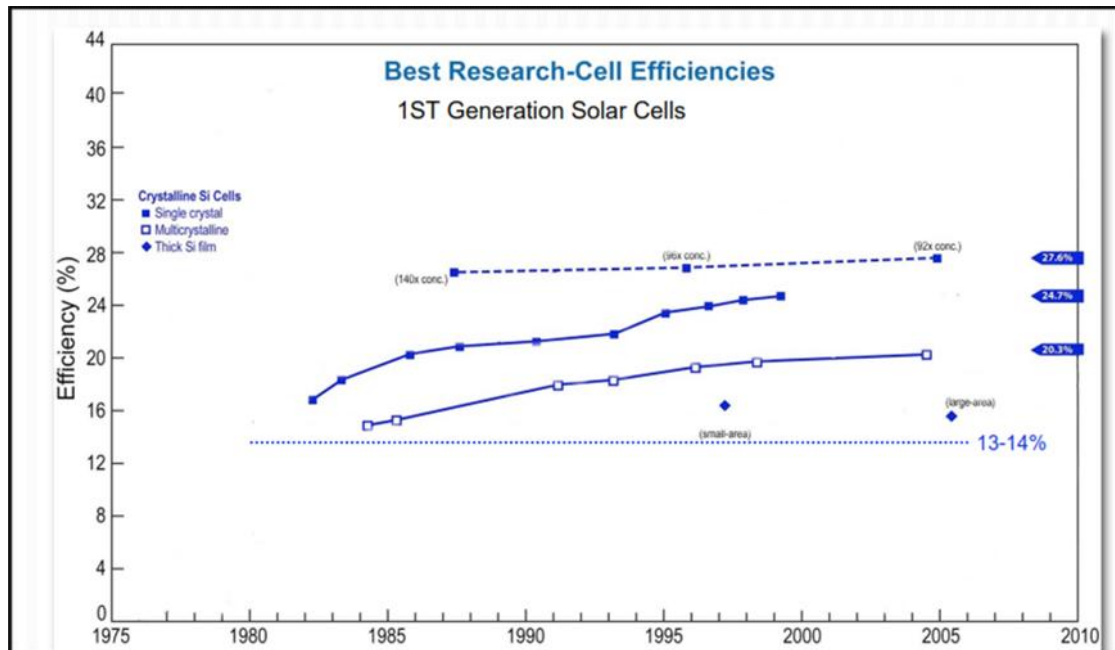


Figure 1.12 1st Generations Solar Cells Efficiency Milestones [5]

2ND Generation Solar Cells: Thin-film Technology Solar Cells:

Because of the high cost of manufacturing of the 1st generation solar cells, a 2nd generation solar cells known as thin film technologies was developed. The technology involves depositing a thin layer of photo-active material (Non-crystalline silicon) onto inexpensive substrates material using plasma enhanced chemical vapor deposition (PECVD) process. Amorphous semiconductor material (a-Si) is commonly used. An amorphous material differs from crystalline material in that there is no long-range

order in the structural arrangement of the atoms. Although the thin film PV cells are less subject to breakage and not vulnerable to most of the other manufacturing problems that are common to the crystalline solar cells, its efficiency is significantly lower. There are also some concerns about the toxic legacy of the materials both in manufacturing and at the end of life. The amorphous solar cells like the one shown in Figure 1.13 below are much flexible to install in that, less support is needed when placing panels on rooftops and it also has advantage of fitting panels on light materials like backpack, textiles etc. The efficiency of thin film technologies solar cell is approaching about 20% based on recent research breakthroughs [5].

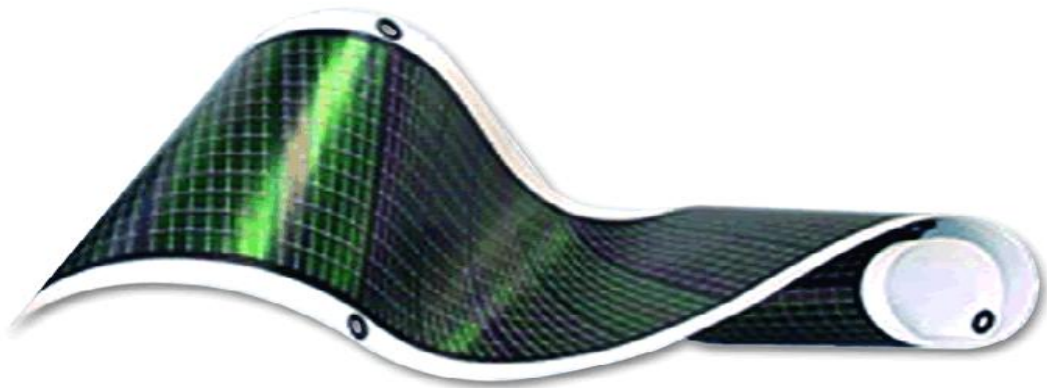


Figure 1.13 Amorphous Solar Cells [21]

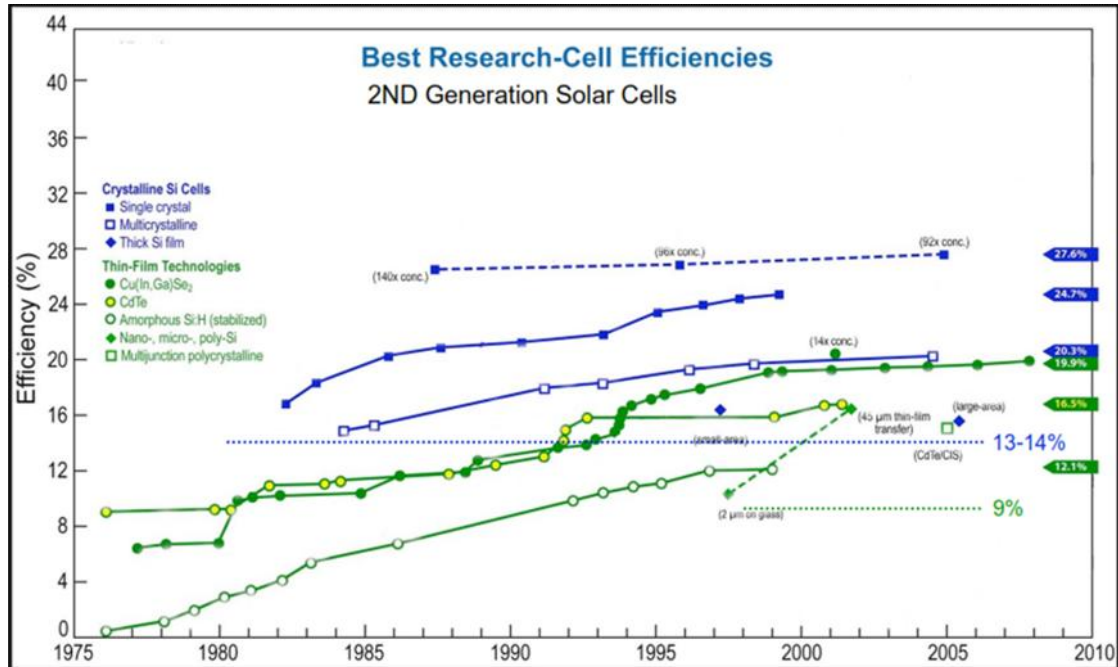


Figure 1.14 2ND Generations Solar Cells Efficiency Milestones [5]

3RD Generation Solar Cells:

The 3rd generation solar cells involve different Semiconductor Technologies that are fundamentally different from the previous semiconductor devices. It has been estimated that 3rd generation solar technologies will achieve higher efficiencies and lower costs than 1st or 2nd generation technologies [6]. Some of these technologies are Nanocrystal Solar Cells, Photo-electrochemical cells, Dye-sensitized hybrid solar cells and Polymer Solar cells. **Nanocrystal solar cell** technology is based on grains of nanocrystals or quantum dots. Examples are Lead selenide (PbSe) semiconductor and Cadmium telluride (CdTe) semiconductor. Quantum dots have band-gaps that are tunable across a wide range of energy levels by changing the quantum dot size. This is in contrast to crystalline materials, where the band-gap is fixed based on the material composition. This property makes quantum dots viable for multi-junction solar cells,

where a variety of different band-gap materials are used to optimize efficiency by harvesting select portions of the solar spectrum. Additional advantages of these cells are; Low-energy and high-throughput processing technologies, low material cost, performs even at low incident light conditions. The disadvantage is that efficiency is still lower than silicon wafer based solar cells and also there is a risk of material degradation overtime [5]. The efficiency of this type of solar cell is approaching about 11% [5]. Please see the Figure 1.15 below for best solar cell research efficiencies to 3rd generation solar cells.

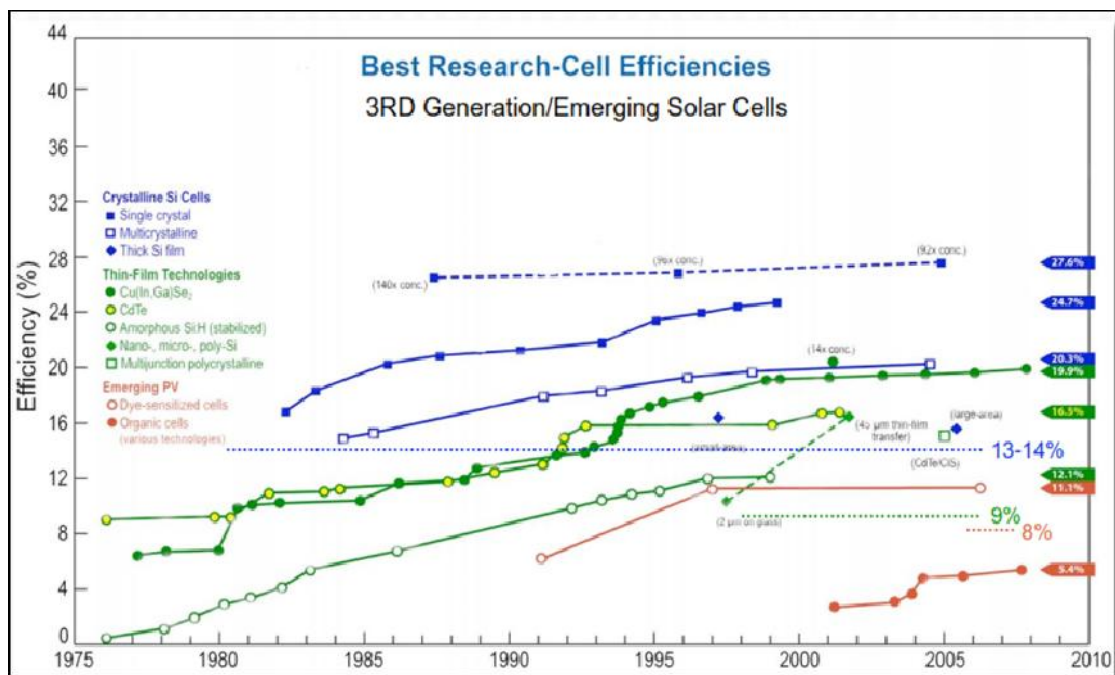


Figure 1.15 3RD Generations Solar Cells Efficiency Milestones [5]

4TH Generation Solar Cells and Future Trend:

This category of solar cells combined the 3rd generation technologies to form the 4th generation solar cells technology. Example is the nanocrystal/polymer solar cell, a Composite photovoltaic cell technology which combines the elements of the solid

state and organic PV cells to form the Hybrid-nanocrystalline oxide polymer composite cell. Although most of these technologies are still in the embryonic development stage, it is predicted that because of the lower cost of material, this type of solar cell would significantly make solar deployment affordable. Another area where Photovoltaic solar cell technology has achieved significant efficiency milestone is in the concentrator solar cell technology. Example is the Multi-junctions (III-Vs) solar cells which has recorded efficiency of greater than 41% [7]. Figure 1.16 below shows best research solar cell efficiency to date, courtesy of NREL (National Renewable Energy Laboratory) and Spectrolab.

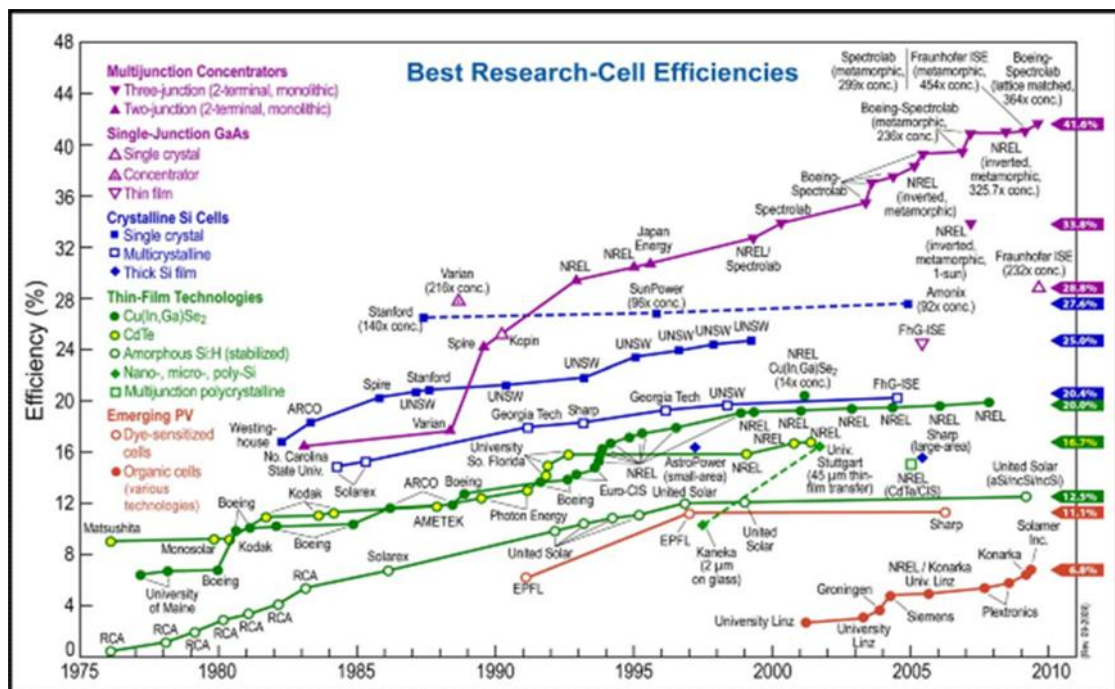


Figure 1.16 Best Research Solar Cells Efficiencies [5]

| Spectrolab Record Efficiency GaInP/ GaInAs/ Ge Cell | |
|--|-----------|
| V_{oc} | = 3.192 V |
| I_{sc} | = 1.696 A |
| FF | = 88.74% |
| V_{mp} | = 2.851 V |
| I_{mp} | = 1.686 A |
| P_{mp} | = 4.805 W |
| Efficiency = 41.6% ± 2.5% | |
| 364.2 suns (36.42 W/cm ²) intensity | |
| 0.3174 cm ² designated area | |
| 25°C, AM1.5D, ASTM G173-03 spectrum | |

Figure 1.17 Record 41.6%-Efficient Concentrator Solar Cells Efficiency [7]

Solar Array Mounting and Tracking

The conversion efficiency of a solar panel is directly proportional to the amount of direct solar irradiance that is absorbed. Irradiance is the amount of solar radiation that strikes the surface of a solar cell or panel and it is expressed in kW/m². The irradiance multiply by time is a measure of solar insolation. The peak sun hours is the number of hours per day when the solar insolation =1kw/m². Apart from the effect of atmospheric attenuations, solar energy absorption is also affected by the earth's distance from the sun and the earth tilt angle with respect to the sun. The angle between the true south and the point on the horizon directly below the sun is the Azimuth angle, measured in degrees east or west of true south. For south facing locations in the northern hemisphere, the default value is an azimuth angle of 180°. Increasing the azimuth angle maximizes afternoon energy production. For a fixed PV

array, the azimuth angle is the angle clockwise from true north that the PV array faces and for a single axis tracking system, the azimuth angle is the angle clockwise from true north of the axis of rotation. The azimuth angle is not applicable for dual axis solar tracking PV arrays. [5]

| Azimuth Angles by Heading | |
|---------------------------|-------------------|
| Heading | Azimuth Angle (°) |
| N | 0 or 360 |
| NE | 45 |
| E | 90 |
| SE | 135 |
| S | 180 |
| SW | 225 |
| W | 270 |
| NW | 315 |

Table 1.2 Azimuth Angle by heading [25]

The sun's height above the horizon is its altitude and it changes based on time and season of the year. Based on the sun's altitude changes, the tilt angle of a solar module with respect to the sun must be carefully considered during module or array installations. The general practice for fixed array is that the tilt angle be equal to the latitude, for providence Rhode Island, the latitude is 41.73° . For better absorption, it is recommended that the tilt angle be adjusted to Latitude + 15° during winter and Latitude - 15° during summer.

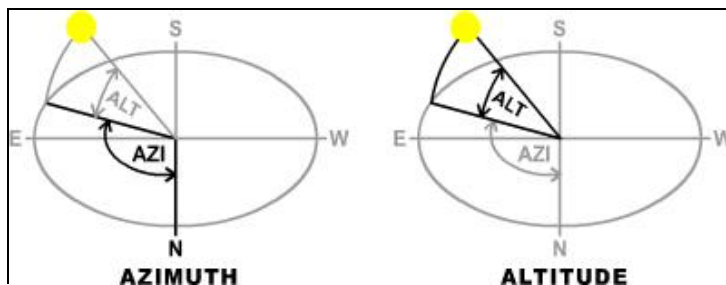


Figure 1.18 Sun's position; Azimuth and Altitude [24]

Solar Tracking

A solar tracker is a device that move or adjust the positional angle of solar photovoltaic panel towards the sun. The sun's position varies both with season and time of day as the sun moves across the sky. Solar panels absorb energy better when orientated perpendicular to the sun, therefore the solar tracker mechanism will essentially increase the effectiveness of solar panels over a fixed solar array or panel.

- Power (W) = VI,
- Irradiance = (W/m²) and
- insolation = W/m²/day

Several factors must be considered when determining the use of trackers. Some of these include: the solar technology being used, the amount of direct solar irradiation available and the cost to install and maintain the trackers among others.

Types of tracker

Trackers can be categorized by the complexity of operation and sophistication.

There are two major groups; Active and passive Trackers. Passive trackers are without motor. Active trackers are motorized and can be sub-categorized into single axis and dual axis trackers:

Single axis

Solar trackers can either have a horizontal or a vertical axis. The horizontal type is used in tropical regions where the sun gets very high at noon, but the days are short. The vertical type is used in high latitudes where the sun does not get very high, but

summer days can be very long. In concentrated solar power applications, single axis trackers are used with parabolic and linear Fresnel mirror designs.

Dual axis

The Dual axis solar trackers have both a horizontal and a vertical axis and thus they can track the sun's apparent motion virtually at any angle. A dual axis tracker maximizes the total power output of solar array by keeping the panels in direct sunlight for the maximum number of hours per day.

Tracker Components:

A typical solar tracking system consist of mechanical parts like the linear actuator with integrated dc or ac motor and gear and an electronic parts like motor drive and controller, sun sensor and power supply. Based on complexity of design and accuracy of tracking, there might be more additional components than those mentioned above. For example, The AZ125 Wattsun dual tracker shown in Figure 1.19 below can move up to 270° in the horizontal direction and up to 75° vertical [23].

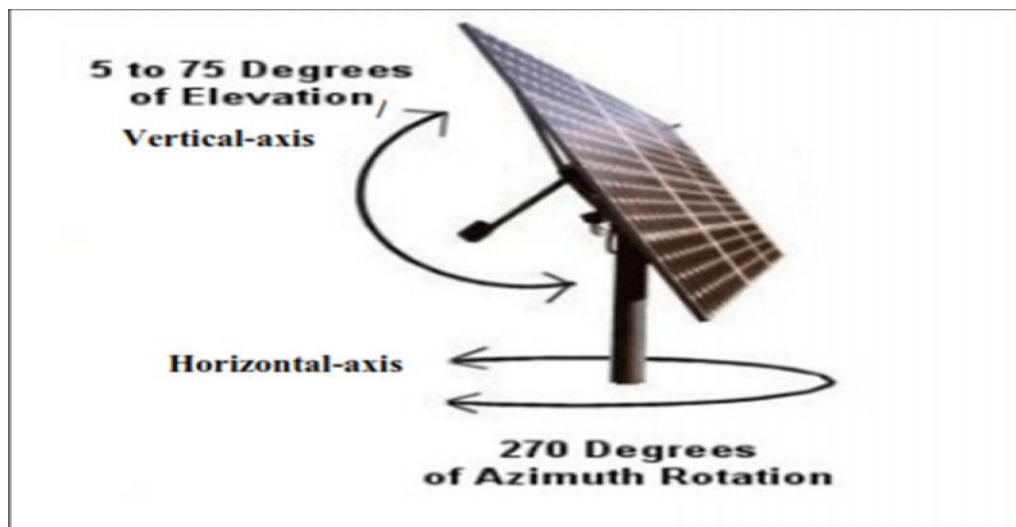


Figure 1.19 A 2-Axis Tracking system [23]

Fixed array Vs Tracked array

A typical solar array with polycrystalline solar cells with 14-18% conversion efficiency would need area of about 7-8m² to produce a 1KW peak power. Some applications does not allow enough space for larger array area but still need to produce sufficient power to meet a desired energy need. Therefore the question of whether to track an array or not is based on specific situation and need. For a fixed Array, the general norm is to install at angle of the Altitude. In the case of Rhode Island region, the Altitude is approximately about 41degree. However, in one of my evaluation of the tilt angle adjustment for a fixed array, I found out that mounting an array at an optimum angle of mount for a stationary array would generate more power than just using the Altitude angle all year round. Figure 1.20 below shows a 30W array that was mounted at the altitude angle as well as at angle slightly higher than the altitude angle under similar environmental conditions during the beginning of winter 2012. The results as shown in the plot of Figure 1.21 shows that mounting at angle slightly higher than the altitude (blue) has about 5% peak power improvement over the altitude tilt angle (green).



Figure 1.20 30W/2.5V solar panel

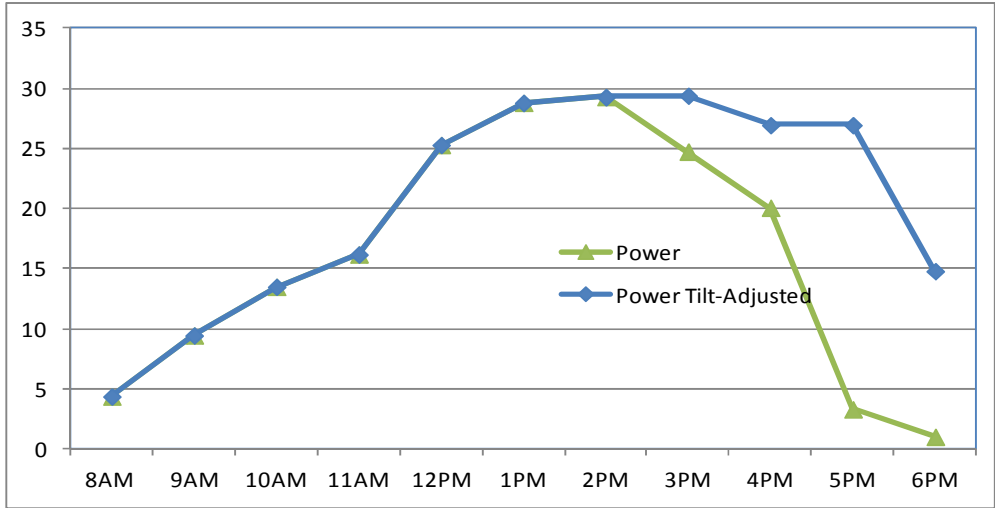


Figure.1.21 Plots of peak power at different tilt angles.

PV-WATTS Modeling:

To further demonstrate the advantage of tracked array over fixed array, the 5KW power system design was also modeled using the PV-Watts simulation tool, which is an Internet-accessible simulation tool for providing quick approximation of the

electrical energy produced by a grid-connected crystalline silicon photovoltaic (PV) system for up to about 239 locations in the US. Users would typically select a location from a station map and set the PV system parameters and the PVWATTS performs an hour-by-hour simulation of monthly and annual alternating current (AC) energy production in kilowatts and energy value in dollars. Some of the system parameters that may be specified include AC rating/size, local electric costs, PV array type (fixed or tracking), PV array tilt angle, and PV array azimuth angle [29]. The tool is available at the National Renewable Energy Laboratory (NREL) website [10]. The results as shown below; proved that the tracked array generates more power (22.8% more) than fixed array.

| Station Identification | | Results | | | |
|--|--------------|---------|--|--------------------|----------------------|
| CellID: | 0273367 | Month | Solar Radiation (kWh/m ² /day) | AC Energy (kWh) | Energy Value (\$) |
| State: | Rhode Island | 1 | 3.10 | 384 | 57.79 |
| Latitude: | 41.8 ° N | 2 | 3.96 | 442 | 66.52 |
| Longitude: | 71.5 ° W | 3 | 4.75 | 569 | 85.63 |
| PV System Specifications | | 4 | 4.75 | 534 | 80.37 |
| DC Rating: | 5.00 kW | 5 | 5.00 | 559 | 84.13 |
| DC to AC Derate Factor: | 0.770 | 6 | 5.20 | 544 | 81.87 |
| AC Rating: | 3.85 kW | 7 | 5.17 | 551 | 82.93 |
| Array Type: | Fixed Tilt | 8 | 5.19 | 556 | 83.68 |
| Array Tilt: | 41.8 ° | 9 | 4.74 | 500 | 75.25 |
| Array Azimuth: | 180.0 ° | 10 | 4.27 | 486 | 73.14 |
| Energy Specifications | | 11 | 3.02 | 345 | 51.92 |
| Cost of Electricity: | 15.1 ¢/kWh | 12 | 2.70 | 327 | 49.21 |
| 5KW SOLAR POWER SYSTEM ANALYSIS : FIXED ARRAY AT 41.8deg Energy = 5797KWH | | Year | 4.32 | 5797 | 872.45 |

Table 1.3 PV-WATTS Simulation of the 5KW Power system: Fixed Array [10]

| Station Identification | | Results | | | |
|---|-----------------|---------|--|--------------------|----------------------|
| CellID: | 0273367 | Month | Solar Radiation (kWh/m ² /day) | AC Energy (kWh) | Energy Value (\$) |
| State: | Rhode Island | | | | |
| Latitude: | 41.8 ° N | | | | |
| Longitude: | 71.5 ° W | | | | |
| PV System Specifications | | 1 | 3.65 | 455 | 68.48 |
| DC Rating: | 5.00 kW | 2 | 4.76 | 535 | 80.52 |
| DC to AC Derate Factor: | 0.770 * | 3 | 5.89 | 714 | 107.46 |
| AC Rating: | 3.85 kW | 4 | 6.07 | 696 | 104.75 |
| Array Type: | 2-Axis Tracking | 5 | 6.81 | 779 | 117.24 |
| Array Tilt: | N/A | 6 | 7.24 | 775 | 116.64 |
| Array Azimuth: | N/A | 7 | 7.22 | 790 | 118.90 |
| Energy Specifications | | 8 | 6.85 | 749 | 112.72 |
| Cost of Electricity: | 15.1 ¢/kWh | 9 | 5.97 | 640 | 96.32 |
| PV-WATTS ANALYSIS: 5KW SOLAR POWER SYSTEM 2-AXIS TRACKING ; Energy=1131.46KWH | | 10 | 5.11 | 590 | 88.80 |
| | | 11 | 3.52 | 405 | 60.95 |
| | | 12 | 3.19 | 389 | 58.54 |
| | | Year | 5.53 | 7518 | 1131.46 |

Table 1.4 PV-WATTS Simulation of the 5KW Power system: 2-Axis Tracker [10]

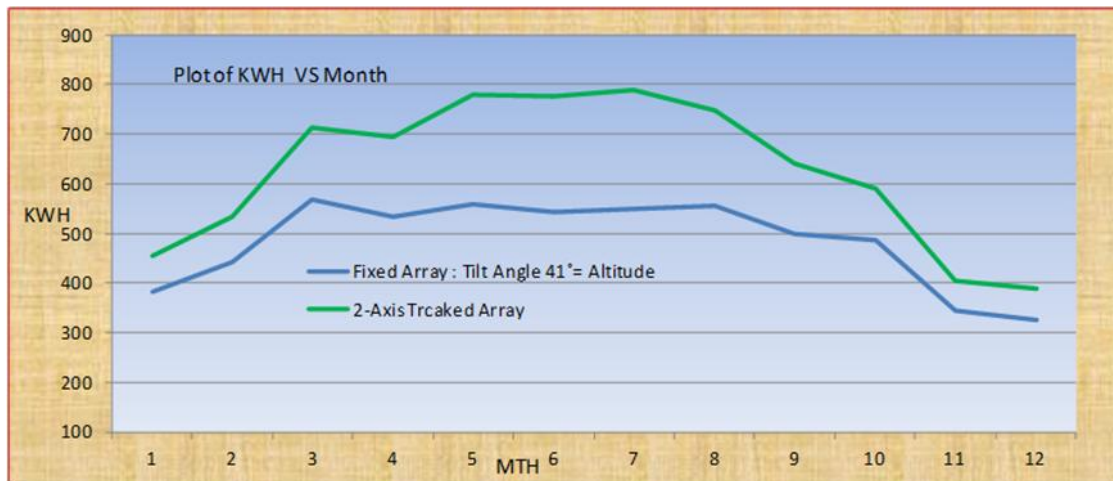


Figure 1.22 PV-WATTS Analysis of the 5KW Project: Fixed Vs 2-Axis Tracker [10]

Array Sizing:

Apart from installing an array for optimum tilt angle, array sizing is also very

important when deploying a solar power system. Photovoltaic power system are sized

based on ; load estimate , inverter system power estimate, wiring sizes, battery and the charge control size estimate (for hybrid or standalone system) and available area. In the 5KW power project for example, (one of the panels we built as shown in Figure 1.24 below) space was not an issue, therefore tracking was not considered. The load demand analysis for the project is as follows and also detailed in table 1.2 below

Load Analysis for the 5KW power system:

From the table, the size of the modules was based on;

The total daily Amp-Hours/day = 1737

Average Sun-hours/day = 5 based on location in Newport RI;

Minimum Power required to meet demand = $P = \frac{1737 \cdot 12}{5} = 4.168\text{KW}$

Because of system losses, it is a general practice to add 20% to minimum power when sizing array; the array size was therefore based on $4.168\text{KW} + 0.2 \cdot 4.168\text{KW} = 5\text{KW}$.

A 12V/294W module would require 17 parallel panels to make 5KW array as shown in the schematic Figure 1.23 below.

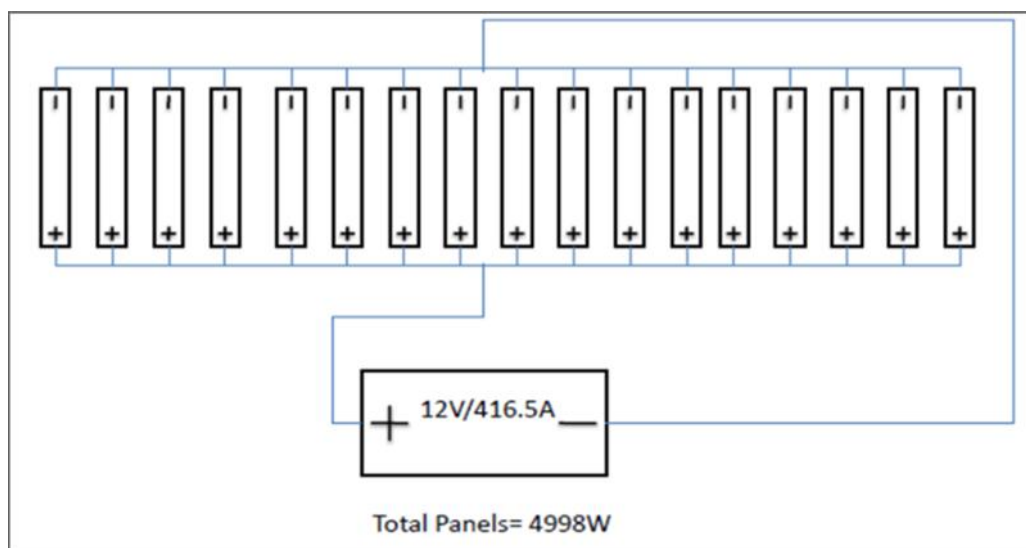


Figure 1.23 Parallel connections of 17 (12V) panels:



Figure 1.24, 12V/294W Hand Made Solar Panel

| URI AND NPNWC 5KW Power System Load Demand | | | |
|--|-----------------|------------------------------|--|
| Load | Avg Current (A) | Average daily Use(hours/day) | Average Daily consumption(AmpIhours/day) |
| Outside Lights | 3.0 | 12.0 | 36.0 |
| Garage doors | 0.5 | 5.0 | 2.5 |
| Water Pump | 11.0 | 4.0 | 44.0 |
| Electric lawn cutter | 3.0 | 2.0 | 6.0 |
| Over-head halogen lamp | 3.0 | 7.0 | 21.0 |
| Alarm system | 2.0 | 7.0 | 14.0 |
| Water Heater | 8.0 | 5.0 | 40.0 |
| Dish-washer | 3.0 | 2.0 | 6.0 |
| Central Fridge and Freezer | 10.0 | 12.0 | 120.0 |
| Plasma TV | 12.0 | 5.0 | 60.0 |
| Home-theater system | 8.0 | 5.0 | 40.0 |
| Electric Stove | 75.0 | 5.0 | 375.0 |
| Satellite-receiver | 5.0 | 3.0 | 15.0 |
| Microwave-oven | 20.0 | 2.0 | 40.0 |
| Desk top and monitors | 4.0 | 5.0 | 20.0 |
| Coffee Maker | 2.0 | 5.0 | 10.0 |
| Laptop and printers | 30.0 | 8.0 | 240.0 |
| Heavy-duty grinder | 20.0 | 5.0 | 100.0 |
| Electric Heater | 40.0 | 8.0 | 320.0 |
| Pressing Iron and steamer | 7.0 | 2.0 | 14.0 |
| Piano | 3.0 | 3.0 | 9.0 |
| Digital Album and Radio | 6.0 | 24.0 | 144.0 |
| Other | 5.0 | 12.0 | 60.0 |
| TOTAL Daily Amp-Ihour Demand | | | 1737 |

Table 1.5 Load Estimate of the 5KW power system

Solar (Photovoltaic) Power System:

Solar power systems can generally be classified according to their functional and operational requirements, component configurations and integration with other power sources and electrical loads. The two principal classifications are grid-tied or utility-interactive systems and stand-alone systems. Photovoltaic systems can be designed to provide DC and/or AC power service, can also operate interconnected with or independent of the utility grid, and can be connected with other energy sources and energy storage systems. Grid-connected or utility-integrated PV systems are designed to operate in parallel with the electric utility grid. The primary component in grid-connected PV systems is the inverter. The photovoltaic inverter system (PVI) converts the DC power produced by the PV array into AC power consistent with the voltage and power quality requirements of the utility grid. The PVI should also automatically stop supplying power to the grid when the utility grid is not energized (Anti-Island requirement). The block flow diagram of a typical grid tied solar power system is shown in the Figure 1.25 below.

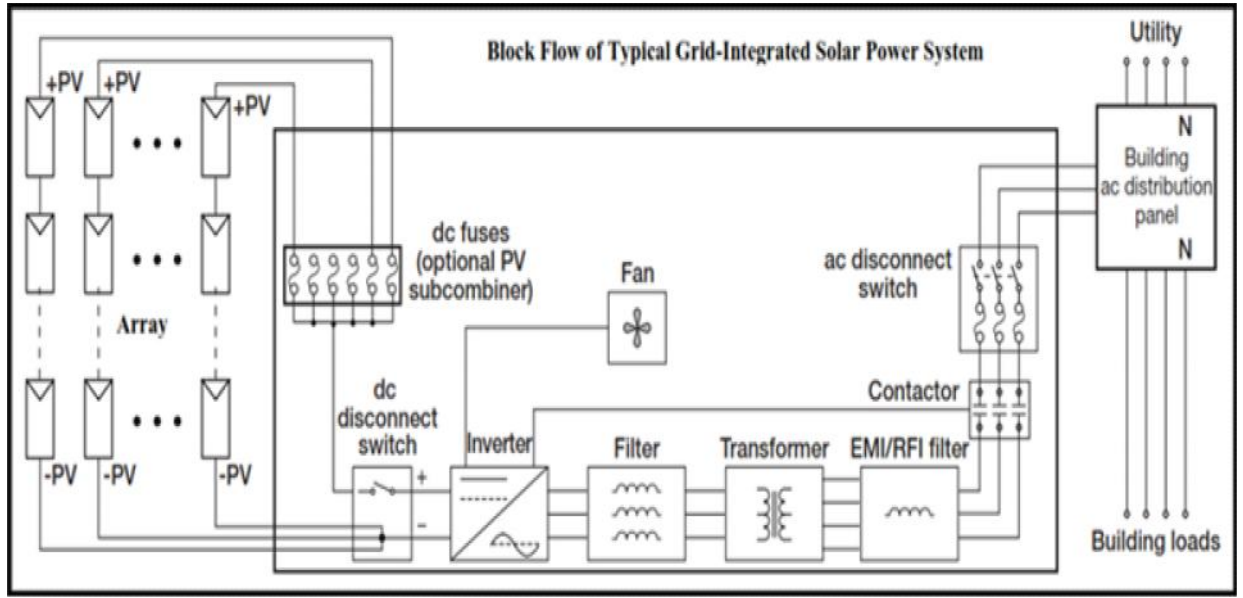


Figure 1.25 Grid Interactive Photovoltaic Power systems [18]

From the Figure above, the DC voltage from the solar power array is fed into the DC-disconnect or string combiner and then to the inverter core. The inverter takes the DC voltage input and performs power conditioning operations through the power electronics switching devices to invert the DC voltage to AC sine wave voltage that is consistent with the voltage and power quality requirements of the utility grid. One key requirement of all grid interactive inverters is that the inverter must be able to recognize and stop operating if the grid is not present either due to fault or in case of utility scheduled service based on IEEE-1547 standard requirements. A bi-directional interface and feedback compatibility is made between the PV system AC output circuits and the electric utility network through the AC disconnects switch and the contactor. This interface also allows the AC power produced by the PV system to either supply on-site electrical loads or to back-feed the grid when the PV power system output is greater than the on-site load demand. At night and or during overcast

situation when the electrical loads are greater than the power output from the PVI, the balance of power required by the load is received from the grid.

Smart Grid Photovoltaic Inverter System (SGPVI):

There are tremendous research going on to refurbish the grid of the future for smartness and efficiency. The 'Smart Grid' concept is still evolving and so also are the standards that defines and qualifies what a smart grid is. Because these standards are yet to mature but still in the developmental stage, it is difficult to ascribe a specific definition to smart grid. However, Smart Grid in the concept of the integration of the electrical and information infrastructures into the utility system can be defined as the incorporation of automation and information technologies with the existing electrical network in order to provide overall improvement to the utility's power reliability and performance. The smart grid would function to deliver increased energy efficiencies and provide significant reduction in carbon emissions and other environmental hazards. It must also provide consumers with the flexibility to manage their energy usage to save money on energy while supporting renewable energy integration. Additional advantage of the smart grid is that it must be intelligent to diagnose power outage and troubleshoot to provide automatic restoration. It must also be able to provide security of the power network system by detecting and reporting network system intruders [30]. Smart Grid total solutions is being driven to provide Assets and Demand Optimization, Smart metering and communications, Distribution and Transmission optimization, and Engineering design optimization [30]. The Smart grid inverter system must therefore be designed to meet these new grid requirements as

specified in the IEEE-1547 standard (Physical and electrical interconnections between utility and distributed generation (DG)) and other standards like ANSI C12.19/MC1219, Advanced metering infrastructure (AMI) etc.

Grid-Integrated Photovoltaic Inverter System:

The process of converting the dc power from the solar array to ac power which can then be used to power industrial or household ac loads or interfaced into the grid is known as inversion. Other than dc-ac inversion, the other major functions or features that are common to most grid-tied solar inverter systems are;

- Maximum power point Tracking,
- Grid integration and disconnection.
- Remote Monitoring

Within the inverter system, dc power from the PV array is inverted or converted to ac power via a set of solid state switches, typically MOSFETs and or IGBTs which essentially switches the dc power back and forth, creating ac (alternating current) power. The arrangement of these semiconductor switches comes in different format known as topology. Figure 1.26 below shows a 2-level 3-phase inverter topology. The inverter electronics power stage consist of 6-IGBT power switches arranged in a 3-phase bridge. By alternately closing the top left and bottom right switches and vice versa of each phase the dc voltage is inverted from positive to negative triangular ac waveforms. These 3-phase waveforms are pulse width modulated to create modified sine waves which are then fed into the line filter inductor and capacitors to smooth out the high frequency components of the modified ac waveforms. The magnitude of the

approximated ac voltage is typically about 208Vac 60HZ line to line which is then fed into the transformer. The transformer serves two major purposes in this configuration; to convert the ac voltage to the correct grid ac voltage both in magnitude and phase angle. The transformer also serves to provide isolation between the grid and the PV. The DC input voltage is typically about 300 -600Vdc in the US and can go up to about 1KV in Europe.

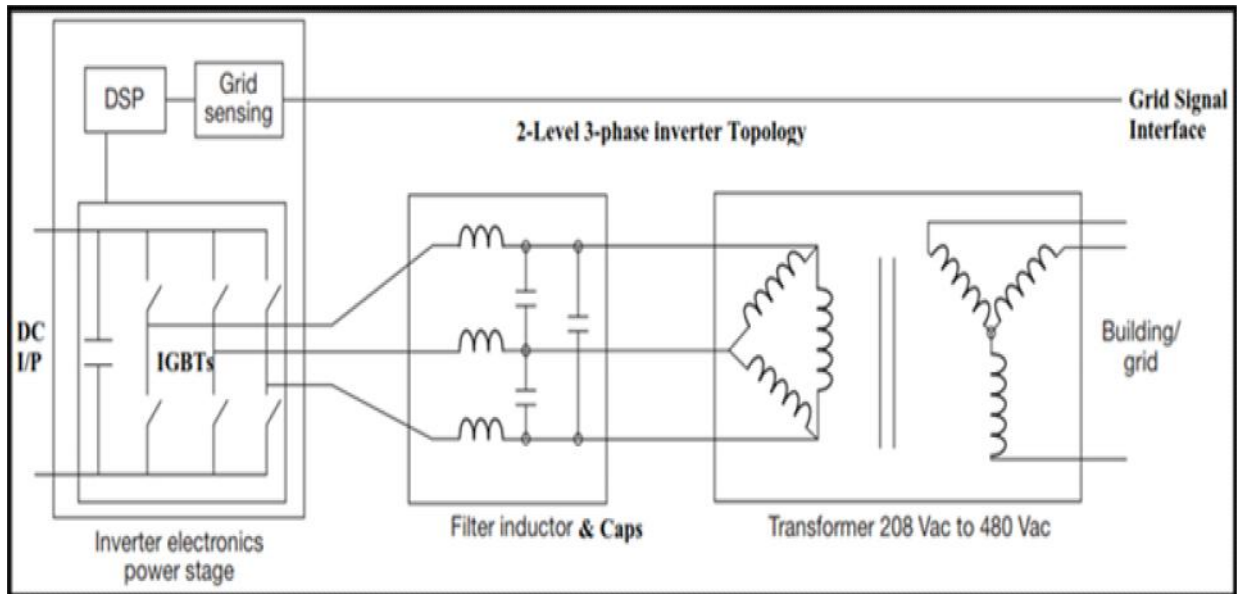


Figure 1.26 2-level 3-phase Inverter Topology [18]

Multi-level Inverter Topology:

Another type of inverter topology is the multi-level inverter. Figure 1.27 below shows a 3-level topology. Each phase has four IGBTs connected in series. The applied voltage on the IGBT is half of a typical conventional two level inverter because of the connection of the series bus capacitors; therefore the topology has the capability of handling higher bus voltage. Other advantages is lower line-to-line and common-mode

voltage steps and lower output current ripple for the same switching frequency as that used in a two level inverter. Because of the staircase waveform characteristics of multilevel inverters, they tend to have reduced electromagnetic compatibility (EMC) issues and lower dv/dt spikes. The basic operation of the circuit below can be explained based on table 1.6 and using a single phase w (Figure 1.28) to demonstrate the switching state and operation of the IGBTs.

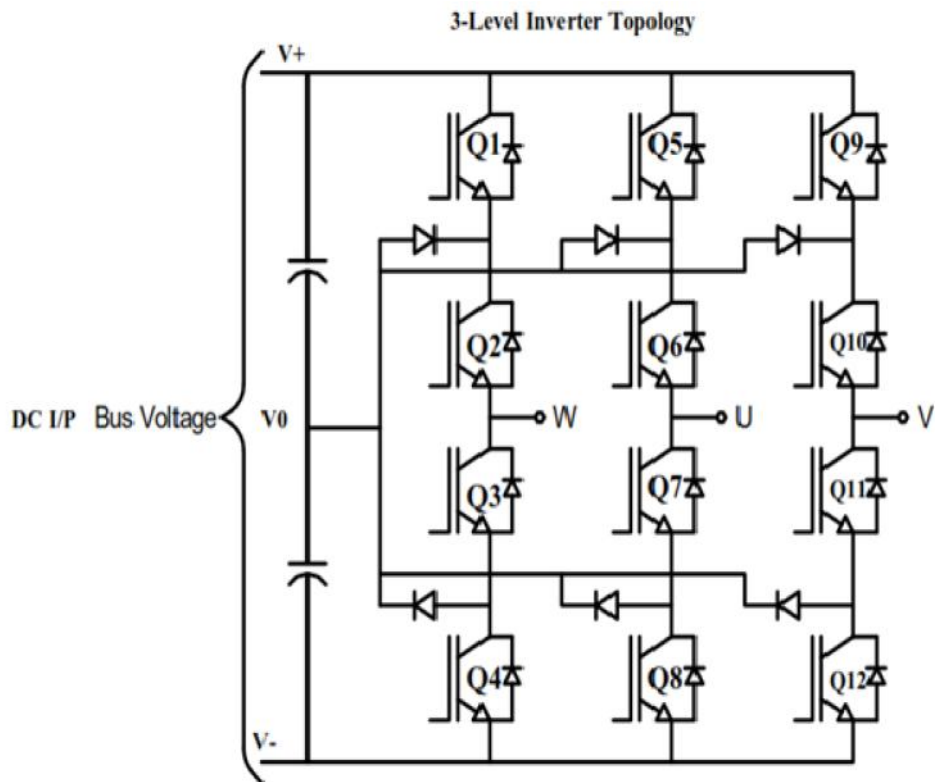


Figure 1.27, 3-level 3-phase Inverter Topology [31]

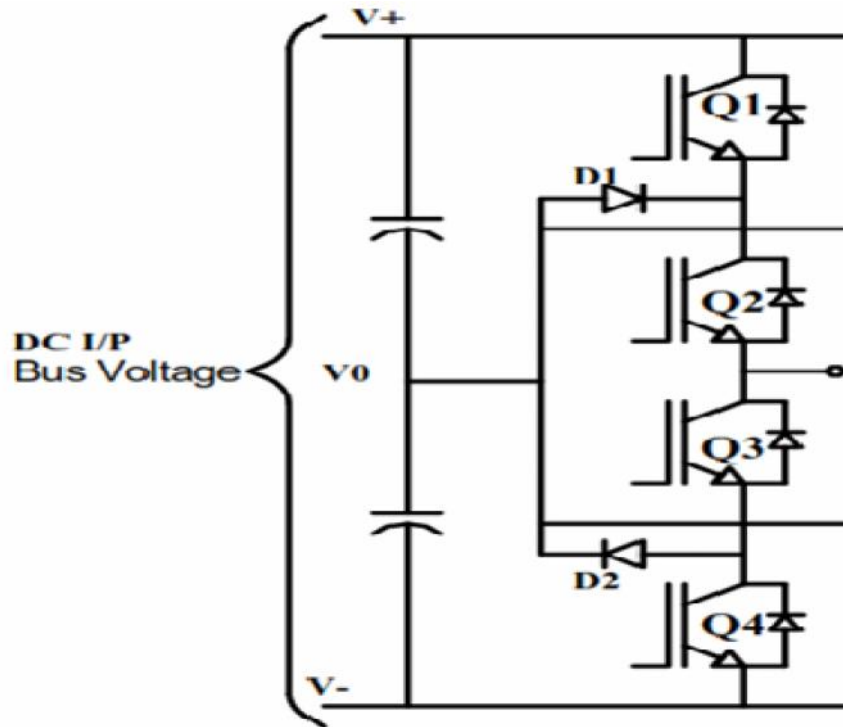


Figure 1.28, 3-level 3-phase Inverter Topology Phase 1 [31]

Output Voltage and Switching States: The 3-level inverter topology produces three different output voltage levels namely; the DC bus voltage $V+$, zero voltage and DC bus negative voltage whereas a two level inverter can only connect the output to either the plus bus or the negative bus. From the Figure 1.28 above and considering the single phase ‘W’ operation; when switch Q1 and Q2 are turned on, the output is connected to $V+$; when Q2 and Q3 are on, the output is connected to $V0$; and when Q3 and Q4 are on, the output is connected to $V-$. From table 1.6, it is shown that Q2 and Q3 would have about 50% duty cycle much longer than Q1 and Q4 which operates at 25% duty cycle. Clamp diodes D1 and D2 provide the connection to the neutral point. Therefore, Q2 and Q3 would have greater conduction loss than Q1 and Q4 but far less switching loss. This topology also has another key advantage, higher efficiency due to

decreased switching losses and also reduced output filter component size and cost as compared to a two level inverter.

| SWITCH | $V_{OUT}=V_+$ | $V_{OUT}=V_0$ | $V_{OUT}=V_-$ |
|--------|---------------|---------------|---------------|
| Q1 | 1 | 0 | 0 |
| Q2 | 1 | 1 | 0 |
| Q3 | 0 | 1 | 1 |
| Q4 | 0 | 0 | 1 |

Table 1.6: Truth table for output voltage and switching states

The Maximum power point tracking (MPPT): The feature that allows an inverter to remain on the ever-moving maximum power point (MPP) of a PV array is called maximum power point tracking (MPPT). As discussed in the section of the solar cell device physics, the IV characteristic curve of PV modules includes the short-circuit current value (I_{sc}) at 0 Vdc, the open-circuit voltage (V_{oc}) value at 0 A and a “knee”, the point where maximum power point (MPP) is found on the curve, this is the location on the IV curve where the voltage multiplied by the current yields the highest value of power. Figure 1.29 shows the MPP for a module at full sun at various temperature conditions. As cell temperature increases, voltage decreases and module conversion efficiency suffers. Other than temperature, module performance is also affected by sun irradiance. When sun is full i.e. at irradiance of $1000W/m^2$, module current is highest and when there is less sunlight, module current decreases and so is conversion efficiency. Since sunlight intensity and module or cell temperature vary substantially throughout the day and the year, array MPP (current and voltage) also varies accordingly. The ability of an inverter to accommodate these environmental variations and optimize its performance to meet grid criteria and other regulatory

standards (NEC, IEEE and UL etc) at all the time of operation is achieved largely due to effective maximum power point tracking feature.

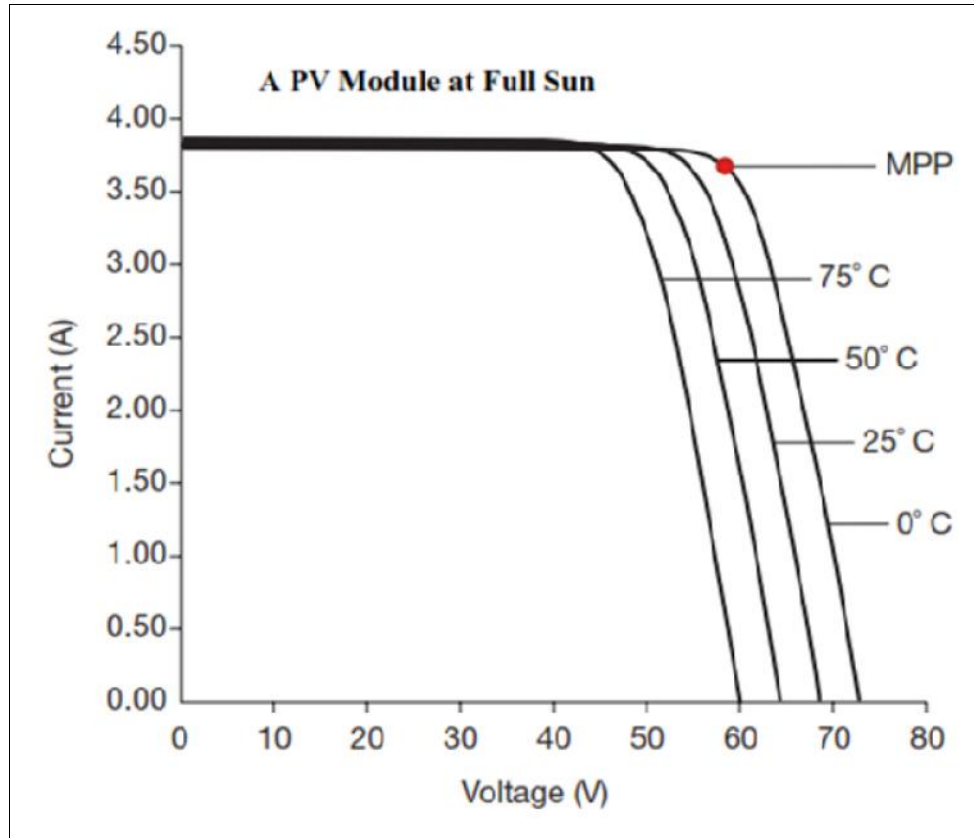


Figure 1.29 MPP on IV-Curve of a PV Module. [18]

Grid integration and disconnection:

All grid-tied solar inverter systems are bound by certain regulatory standards.

Typically in the US, these standards are defined by bodies like the IEEE, UL (Underwriter Laboratory) and NEC (National Electrical Codes) NEC. The standards that govern grid-tied photovoltaic inverter systems are UL 1741 and IEEE 1547. One of the critical requirements of these standards is that all grid-tied inverters must disconnect from the grid if the ac line voltage or frequency goes above or below limits

prescribed in the standard. See the table 1.7 below for such limits [18]. Also if the grid is not present due to a fault or for some other reasons, the inverter must shut down to avoid the solar power system of being an island. In any of these cases, the solar inverter system must not interconnect or feed power into the grid until the inverter is sure that proper utility voltage and frequency is recorded at the grid for a period of 5 minutes. This is to protect against the inverter feeding power into the grid during a fault or during a utility scheduled maintenance exercise.

| Inverter type, size and voltage | Voltage range [V] | Clearing time(s) (seconds) | Frequency range [Hz] | Clearing time(s) (seconds) |
|--|---------------------|----------------------------|----------------------|----------------------------|
| Residential 240 Vac | $V < 211.2$ | 2.00 | $f > 60.5$ | 0.16 |
| | $211.2 < V < 264$ | operational | $f < 59.3$ | 0.16 |
| | $264 < V$ | 1.00 | $59.3 < f < 60.5$ | operational |
| Commercial, 3-phase 208 Vac, <30 kW inverter | $V < 104$ | 0.16 | $f > 60.5$ | 0.16 |
| | $104 < V < 183$ | 2.00 | $f < 59.3$ | 0.16 |
| | $183 < V < 228.8$ | operational | $59.3 < f < 60.5$ | operational |
| | $228.8 < V < 249.6$ | 1.00 | — | — |
| | $249.6 < V$ | 0.16 | — | — |
| Commercial, 3-phase 480 Vac, >30 kW inverter | $V < 240$ | 0.16 ¹ | $f > 60.5$ | 0.16 |
| | $240 < V < 422.4$ | 2.00 ¹ | $57.0 < f < 59.8$ | 0.16 ¹ |
| | $422.4 < V < 528$ | operational | $f < 57.0$ | 0.16 |
| | $528 < V < 576$ | 1.00 ¹ | $59.8 < f < 60.5$ | operational |
| | $576 < V$ | 0.16 ¹ | | |

Table 1.7: Utility grid voltage and frequency limits for grid-tied PV: [18]

Monitoring and Communications:

The interactions of the various components that make up the solar power systems namely; The Grid, Inverter, and the solar array and all the various components and interconnect are achieved by effective software and monitoring communication

gadgets. For example looking at Figure 1.26 above, to reliably control the inverter, the software designed to run on the inverter's digital signal processor which controls the PWM waveforms and other feedback signals to and from the grid must function to meeting all the appropriate UL 1741 and IEEE 1547 safety requirements. Another important function of the software and monitoring portion of the system is the controls of the MPPT features that vary the dc voltage and current level as appropriate to accurately and quickly follow the moving MPP of the PV array. Software is also used to drive the contactor that connects the inverter to the grid in the morning and remove it from the grid at night when the sun goes out.

The Key Components of a Grid-Tied Photovoltaic inverter system:

Looking at Figure 1.26 above, some of the critical components of an inverter systems are: solid state switches i.e. IGBTs and or MOSFETs which are used to invert the DC voltage into ac voltage. Other key components in the main power inversion circuit are line inductors, capacitors and power transformer. The design selection of these critical components is very important for the efficient operation of the solar power system.

IGBT Module:

The IGBT, Insulated Gate Bipolar Transistor, is a solid state switching transistor that combines the collector-emitter voltage characteristics of a bipolar transistor and the drive characteristic of a MOSFET. It is controlled by voltage applied to the gate terminal. The IGBT, MOSFET and BJT are all solid state devices that can be used in switching applications. A brief comparison between the structures of these solid state

switching devices is that; The NPN BJT is a three junction device that requires a continuous current flowing into the base region to operate the junctions to conduct current. Whereas MOSFET and the IGBT are voltage controlled devices, they only require voltage on the gate to maintain conduction through the device. The IGBT has one junction more than the MOSFET, and this junction allows higher blocking voltage and conductivity modulation for reduced on-state conduction losses. The additional junction in the IGBT does however limit switching frequency during conduction. MOSFET does not have this switching speed limitation. Inverters IGBT modules must be designed to be rugged, low loss and low on-state saturation voltages and must also be able to maintain a relatively high switching speed, up to 20KHZ with less loss. A typical IGBT module and schematic from POWEREX [26] is shown below.

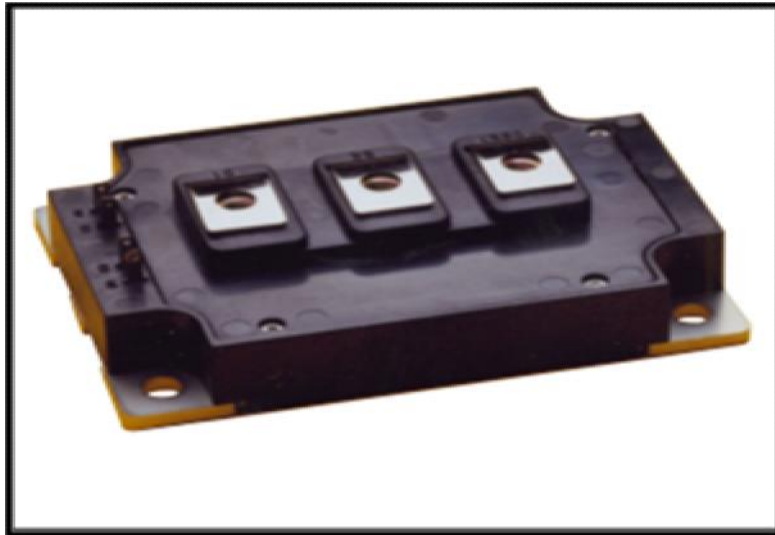


Figure 1.30 Powerex 600A/600V Dual IGBT Module [26]

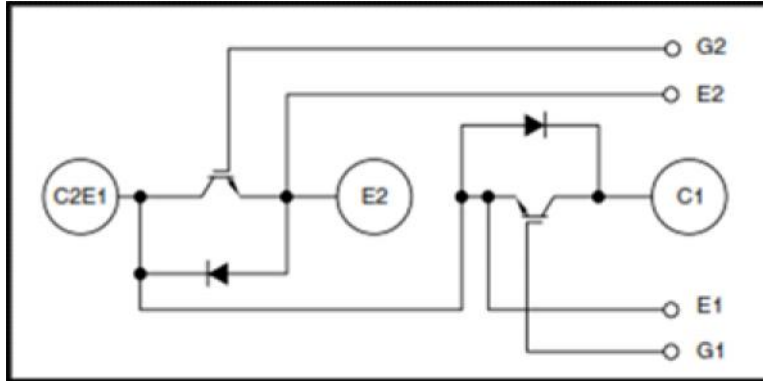


Figure 1.31 Powerex 600A/600V Dual IGBT schematic [26]

Power Magnetics:

Another very critical portion of the Grid-tied solar inverter system is the power magnetic components, Line inductor and transformer.

Inductor: The function of the inductor is to smoothen out the raw and noisy triangular waveform of the pulse width modulated power switches. From Figure 1.26 the line inductors and the filter capacitors clean out the high frequency harmonics before passing the waveforms through the transformer. The IEEE 1547 requires that the current harmonics of grid-tied photovoltaic inverters be less than 5% THD and voltage harmonics less than 2% THD. The main component that helps the inverter achieve these requirements is the inductor. A snap picture of the harmonics measurements on a Yokogawa power analyzer and data of power quality characteristic of a grid-tied inverter system that I worked on during the course of this thesis is as shown in Figure 1.32 below. As seen from the Figure, the current THD is about 2.1% and the Voltage THD about 0.4% well below the requirement. A high level of harmonics could be a sign that the inductor is not efficient since harmonics are losses. Some other key

specification of power line inductor is low winding temperature rise and low dc resistance. Insulation class should be N or R (200 to 220°C). Another key feature of a good inductor is low acoustic noise typically below 50dB at full load. Inductor construction is also very important, there must be proper insulation between the laminations and the core brackets and other supporting structures to avoid close eddy current loop. Figure 1.33 shows the actual physical picture of the line inductor.

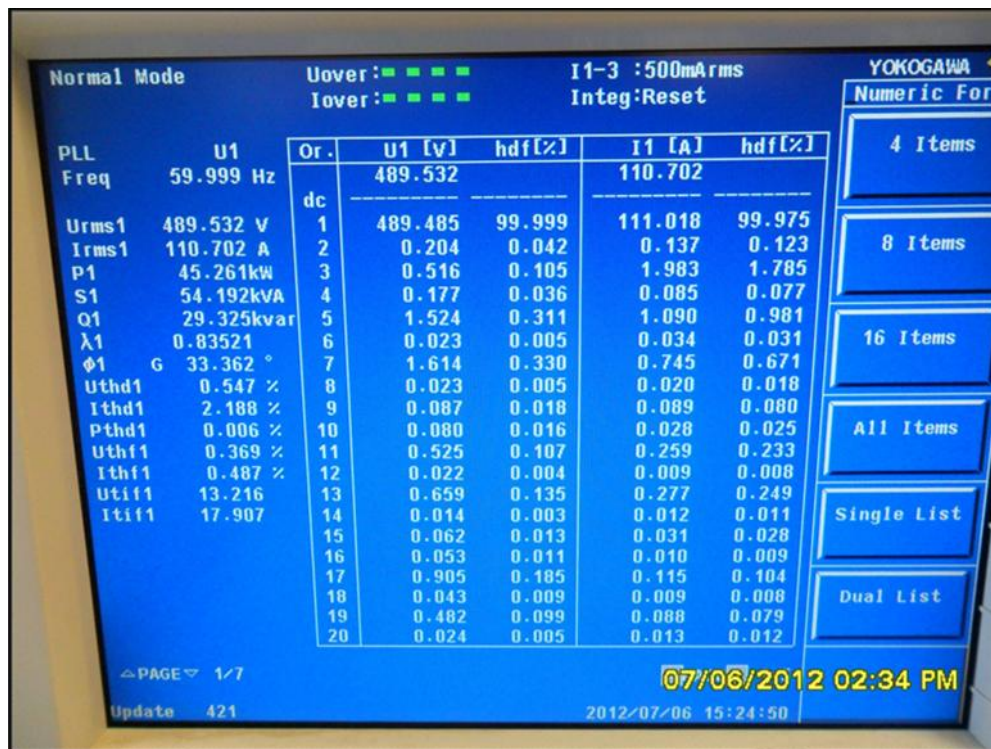


Figure 1.32 Harmonics of a 3-phase Grid-tied Inverter system.



Figure 1.33, 3-Phase 300A Line Inductor

Transformer:

The main function of the transformer in a grid-tied solar power system is to convert the ac input voltage from the inverter core to the correct grid ac voltage both in magnitude and phase angle typically 208Vac RMS or 480V RMS Delta-Wye depending on configuration. The transformer also serves to provide isolation between the grid and the PV. The efficiency of the power magnetic (transformer and Inductor) is key to the efficiency of the solar power system. Some of the key specifications that define an efficient transformer are; very low No-load and Load losses, low winding temperature rise, good dielectric voltage withstand, good load regulation less than 1.5%, ability to withstand transient overvoltage situation up to 120% of rated voltage without saturation and no excessive audible noise (IEEE-1547). The efficiency of grid-tied inverter system is typically measured using the CEC (California Energy

Commission) efficiency model. The CEC models basically assign weighted values based on load levels and then the cumulative of all the load levels would be the overall efficiency. One of such transformer that I tested was a 100KVA 208/480V delta-wye transformer with a CEC efficiency spec on the name plate of 99.30% at 40 degree C ambient temperature, the physical picture is shown in Figure 1.34 below.



Figure 1.34: Snap picture of a 3-Phase 100KVA Transformer under test.

CHAPTER 4

FINDINGS

This research has changed my perspective about renewable energy in general and has given me a tremendous practical intuition about solar power system in particular. Solar cells development has come a long way and yet, it appears the technology is far from perfection judging from the fact that the best solar cell conversion efficiency for commercially available solar cells is still in the 20% range. While solar cell technology has evolved over the years, one thing I found out is that tremendous research and breakthrough are still going on year after year to perfect the breakthrough of the past and lay the foundation for the next generation solar cells. I was also able to leverage the opportunity that I have as an engineer working in one of the most dynamic industry (Renewable Energy) of this time. I had the opportunity to visit solar farms and experience firsthand how solar power system works and how they are integrated into the grid system. I was also able to experience the detail that goes into the design and the manufacturing processes that are peculiar to solar inverter system and the various regulatory (national and International) standards that a particular solar power system must meet. Having been assigned to one of the key aspect of the business, component engineering, the research prepared me to dig deep into the various components like the Dry-type Power Transformers, Power Line Reactors or Inductors, Power Film capacitors, IGBTs, Power MOSFET, and Power supplies among others that goes into the solar inverter system and how their performance

specifications affects the overall efficiency of the solar power system. This thesis has also shown with empirical data the energy and cost benefits of good array mounting and also the advantages of tracked array vs. fixed arrays. Finally, additional studies are needed to fully understand the scope of smart grid as it relates to solar photovoltaic power system.

CHAPTER 5

CONCLUSION

My thesis has presented detailed solar photovoltaic power system technology starting with the solar cell device physics and its principle of operation, to solar cell efficiency and sources of losses to how to mitigate the losses. I have also detailed various types of solar cell from the initial discovery (1st generation) to the present technological breakthroughs and future trend. The solar photovoltaic inverter system and the key components that ensure efficient operation were also detailed. Based on this research and judging from the outstanding breakthroughs that have been made in the technology of solar cells in the last couple of decades, the future trend looks optimistically bright for solar photovoltaic applications. The ongoing technology and research in the 3rd and 4th generation solar cells would no doubt transform solar energy from niche to mainstream in the very near future. Other factors that are catalyst to transforming this renewable source of energy is the increasing cost of fossil fuel and climate change awareness.

This thesis has also presented details of the various regulatory standards that a grid-tied solar power system must meet and the challenges involved in meeting these requirements. The thesis has shown that to achieve an efficient solar power system, it must start from the solar cell/module selection phase. Optimum mounting angle and the use of tracking where necessary to capture more sunlight is also an effective way to maximize efficiency. It also requires efficient photovoltaic inverter system with

effective MPPT features. Key components of the inverter like the power switches, magnetic components must be properly selected for optimum performance. Lastly, this thesis has provided in detail the various ways to improve the efficiency of a solar power system from the solar cell structure to the array to the DC-AC inversion and grid interconnection. From the foregoing, improving solar power system efficiency involves careful consideration of all the various portion of the entire solar power system.

BIBLIOGRAPHY

- [1] Green, Martin A. Solar Cells; Operating Principles, Technology, and System Applications, Prentice-Hall Inc, 1982 pp xii and pp 62-184
- [2] http://upload.wikimedia.org/wikipedia/commons/4/4c/Solar_Spectrum.png:
Date accessed: 3/11/13
- [3] <http://solarsystem.nasa.gov/planets/profile.cfm?Object=Sun&Display=Facts>:
Date accessed: 3/11/13
- [4] [http://en.wikipedia.org/wiki/Air_mass_\(solar_energy\)](http://en.wikipedia.org/wiki/Air_mass_(solar_energy)) Date accessed: 3/11/13
- [5] The National Renewable Energy Laboratory (NREL Web page):
<http://www.nrel.gov/ncpv/index.html> Date accessed: 10/11/12 and
http://www.nrel.gov/ncpv/images/efficiency_chart.jpg:Date accessed: 10/11/12
- [6] http://en.wikipedia.org/wiki/Cost_of_electricity_by_source#Photovoltaics:
Date accessed: 2/4/13
- [7] R. R. King et al., 24th European Photovoltaic Solar Energy Conf., Hamburg, Germany, Sep. 21-25, 2009, Available at
http://www.spectrolab.com/DataSheets/PV/pv_tech/Evolution%20of%20Multi%20junction%20Technology.pdf Date accessed: 2/3/13
- [8] Martin A. Green, Keith Emery, Yoshihiro Hishikawa, Wilhelm Warta and Ewan D. Dunlop; Solar cell efficiency tables (version 41), Progress in Photovoltaics: Research and Applications; Wiley Online Library, available at
<http://onlinelibrary.wiley.com/doi/10.1002/pip.2352/pdf> Date accessed: 4/2/13
- [9] www.pwr.com Date accessed: 1/29/13
- [10] http://gisatnrel.nrel.gov/PVWatts_Viewer/index.html Date accessed: 4/11/13
- [11] http://www.smartgrid.gov/the_smart_grid Date accessed: 2/1/13
- [12] <http://arraytechinc.com> Date accessed: 2/2/13
- [13] <http://www.ieee-pes.org/> Date accessed: 12/1/12
- [14] http://www.eere.energy.gov/basics/renewable_energy/pv_cells.html
Date accessed: 4/20/13
- [15] http://en.wikipedia.org/wiki/Solar_cell Date accessed: 12/10/12

- [16] http://www.eecis.udel.edu/~honsberg/Eleg620/04_pn%20junctions.pdf
Date accessed: 12/10/12
- [17] Green, Martin A. Solar Cells; Operating Principles, Technology, and System Applications, Prentice-Hall Inc, 1982 pp 85-100
- [18] Worden, James and Zuercher, Michael M.; How Inverters Work, Solar Pro, issue 2.3 April/May 2009 http://solarprofessional.com/articles/products-equipment/inverters/how-inverters-work?v=disable_pagination Date accessed: 2/2/11
- [19] Upadhyaya, Ajay; Yelundur, Vijay; Rohatgi, Ajeet: High Efficiency Monocrystalline Solar Cells With Simple Manufacturing Technology: 21st European Photovoltaic Solar Energy Conference and Exhibition, Dresden, Germany; September 4-8, 2006
- [20] Sheoran, Manav; Upadhyaya1, Ajay; Rounsaville, Brian etc , Investigation of The Effect of Resistivity and Thickness on The Performance of Cast Multicrystalline silicon solar cells : 4th World Conference on Photovoltaic Energy Conversion , Hawaii, USA; May 7-12, 2006
- [21] <http://www.solarcell.net.in/thin-film-solar-cells/> Date accessed: 10/20/12
- [22] <http://www.newport.com/Introduction-to-Solar-Radiation/411919/1033/content.aspx> Date accessed: 10/20/12
- [23] <http://www.soldist.com/products/racking/wattsun/> Date accessed: 10/10/12
- [24] http://wiki.naturalfrequency.com/wiki/Solar_Position Date accessed: 10/8/12
- [25] <http://en.wikipedia.org/wiki/Azimuth> Date accessed: 12/1/12
- [26] POWEREX 600V/600A Dual IGBT Module Datasheets-
http://www.pwr.com/pwr/docs/cm600dy_12nf.pdf Date accessed: 10/7/12
- [27] Illinois.edu Engineering portal web site:
<https://wiki.engr.illinois.edu/download/attachments/220434772/CH4SolarCellOperationalPrinciples.pdf?version=1&modificationDate=1365447090000>
Date accessed: 10/1/12
- [28] Purnomo Sidi Priambodo, Nji Raden Poespawati and Djoko Hartanto (2011). Solar Cell, Solar Cells – Silicon Wafer-Based Technologies, Prof. Leonid A. Kosyachenko (Ed.), ISBN: 978-953-307-747-5, InTech, Available from:
<http://www.intechopen.com/books/solar-cells-silicon-wafer-based-technologies/solar-cell> Date accessed: 2/27/13

- [29] B. Marion and M. Anderberg. "PVWATTS-An Online Performance Calculator for Grid-Connected PV Systems," in Proceedings of the ASES Solar 2000 Conference, June 16-21, 2000, Madison, WI.
- [30] John McDonald, GE Energy Digital Energy: IEEE PES Boston; Smart Grid Series May, 2012 Session 1 and 2
- [31] Introduction to Three Level Inverter (TLI) Technology Applications notes available at:
<http://www.pwr.com/pwr/app/TLI%20Series%20Application%20Note.pdf>
Date accessed: 4/2/10